micromachines

MDPI

Article

Catalytic Hydrolysis of Phosphate Monoester by Supramolecular Complexes Formed by the Self-Assembly of a Hydrophobic Bis(Zn^{2+}-cyclen) Complex, Copper, and Barbital Units That Are Functionalized with Amino Acids in a Two-Phase Solvent System

Yuya Miyazawa [1], Akib Bin Rahman [1], Yutaka Saga [1], Hiroki Imafuku [1], Yosuke Hisamatsu [1] and Shin Aoki [1,2,*]

[1] Faculty of Pharmaceutical Sciences, Tokyo University of Science, 2641 Yamazaki, Noda, Chiba 278-8510, Japan
[2] Research Institute for Science and Technology, Tokyo University of Science, 2641 Yamazaki, Noda, Chiba 278-8510, Japan
* Correspondence: shinaoki@rs.noda.tus.ac.jp; Tel.: (+81)-4-7121-3670

Received: 16 June 2019; Accepted: 1 July 2019; Published: 4 July 2019

Abstract: We previously reported on the preparation of supramolecular complexes by the 2:2:2 assembly of a dinuclear Zn^{2+}-cyclen (cyclen = 1,4,7,10-tetraazacyclododecane) complex having a 2,2′-bipyridyl linker equipped with 0~2 long alkyl chains (Zn_2L^1~Zn_2L^3), 5,5-diethylbarbituric acid (Bar) derivatives, and a copper(II) ion (Cu^{2+}) in aqueous solution and two-phase solvent systems and their phosphatase activities for the hydrolysis of mono(4-nitrophenyl) phosphate (MNP). These supermolecules contain $Cu_2(\mu\text{-}OH)_2$ core that mimics the active site of alkaline phosphatase (AP), and one of the ethyl groups of the barbital moiety is located in close proximity to the $Cu_2(\mu\text{-}OH)_2$ core. The generally accepted knowledge that the amino acids around the metal center in the active site of AP play important roles in its hydrolytic activity inspired us to modify the side chain of Bar with various functional groups in an attempt to mimic the active site of AP in the artificial system, especially in two-phase solvent system. In this paper, we report on the design and synthesis of new supramolecular complexes that are prepared by the combined use of bis(Zn^{2+}-cyclen) complexes (Zn_2L^1, Zn_2L^2, and Zn_2L^3), Cu^{2+}, and Bar derivatives containing amino acid residues. We present successful formation of these artificial AP mimics with respect to the kinetics of the MNP hydrolysis obeying Michaelis–Menten scheme in aqueous solution and a two-phase solvent system and to the mode of the product inhibition by inorganic phosphate.

Keywords: supramolecular chemistry; zinc; copper; hydrolysis; dephosphorylation; self-assembly

1. Introduction

The regulation of protein phosphorylation and dephosphorylation is an important process in terms of cellular signal transduction, apoptosis, and the cell cycle among other issues. The phosphorylation of proteins is mediated by protein kinases, such as tyrosine kinases which are related to signal transduction pathways in living cells [1]. Indeed, several molecular targeted drugs that target tyrosine kinases in cancer cells and inhibit their action have been developed for the treatment of cancer [2,3]. On the other hand, dephosphorylation is promoted by the action of protein phosphatases such as alkaline phosphatase (AP) which contains two Zn^{2+} ions in its active center [4–10]. Although some artificial

phosphatases that mimic the active center of metallophosphatases have been reported [11–22], very few of them function as catalysts for the hydrolysis of a phosphate monoester such as mono(4-nitrophenyl) phosphate (MNP). Hence, dephosphorylation by artificial catalysts that mimic protein phosphatases remains a great challenge.

It has been described that chemically synthesized enzyme models have several disadvantages including, (i) a lack of long-range interactions between catalysts and substrate and/or between functional groups in their active sites, (ii) the synthesis of such compounds is time-consuming, and (iii) they are active only in organic solvents in many cases [23]. Indeed, the synthesis of artificial enzyme models that are constructed by covalent bonds require long and complex synthetic routes especially for their functionalization, as a result, only a limited number of structures have been reported. These drawbacks, however, could be overcome by a supramolecular strategy utilizing the self-assembly of the artificial and functionalized molecular building blocks that are readily available [24–52].

In this context, we previously reported on the formation of the supramolecular complex **8a**, by the 2:2:2 assembly of a bis(Zn^{2+}-cyclen) complex (cyclen = 1,4,7,10-tetraazacyclododecane) containing 2,2′-bipyridyl (bpy) linker **1** (Zn_2L^1), a dianion of barbital **4a** (Bar), and a copper(II) ion in an aqueous solution which is stabilized by non-covalent bonds (Scheme 1a) [19,24]. The X-ray crystal structure of the supermolecule **8a** revealed that it contains a $Cu_2(\mu\text{-}OH)_2$ core, which resembles the active centers of metallophosphatases such as AP, and that one of the ethyl groups of the Bar unit is located in close proximity to the $Cu_2(\mu\text{-}OH)_2$ core [24]. More importantly, **8a** accelerates the hydrolysis of MNP, although the yield is low, possibly due to product inhibition by inorganic phosphate (HPO_4^{2-}), a byproduct of the MNP hydrolysis.

We also reported on the formation of the hydrophobic supramolecular complexes **9a–c** and the amphiphilic supramolecular complexes **10a–c** (Scheme 1a) by the 2:2:2 assembly of a hydrophobic bis(Zn^{2+}-cyclen) complex containing two long alkyl chains **2** (Zn_2L^2) and a complex that contained one long alkyl chain **3** (Zn_2L^3), respectively, with Bar^{2-} derivatives and Cu^{2+} in a two-phase solvent system ($CHCl_3/H_2O$) [53,54]. As shown in Scheme 2, we expected that the hydrophobic or amphiphilic 2:2:2 complexes **9** or **10** would be formed mainly in the organic layer, and that product inhibition by HPO_4^{2-} could be avoided, since the hydrophilic HPO_4^{2-} would be released into the aqueous layer, thus permitting the $Cu_2(\mu\text{-}OH)_2$ core to be regenerated. The results showed that **9** and **10** accelerated the hydrolysis of MNP and one of most important findings was that the hydrolysis of MNP by **9** and **10** in the two-phase solvent system obeyed Michaelis–Menten kinetics, suggesting that these reaction systems consisting of a supramolecular complex in two-phase solvent system closely mimic the active sites of AP. However, catalytic activity was observed only in the case of **10** (the catalytic turnover numbers (CTN) were 3~4 [54]), but not in **9** [53]. In addition, the product inhibition of **9** and **10** by inorganic phosphate (HPO_4^{2-}) was not competitive, although it is well known that HPO_4^{2-} inhibits natural AP in a competitive manner. These results raised next question of how to design and synthesize good and appropriate models for natural enzymes such as AP based on a supramolecular strategy.

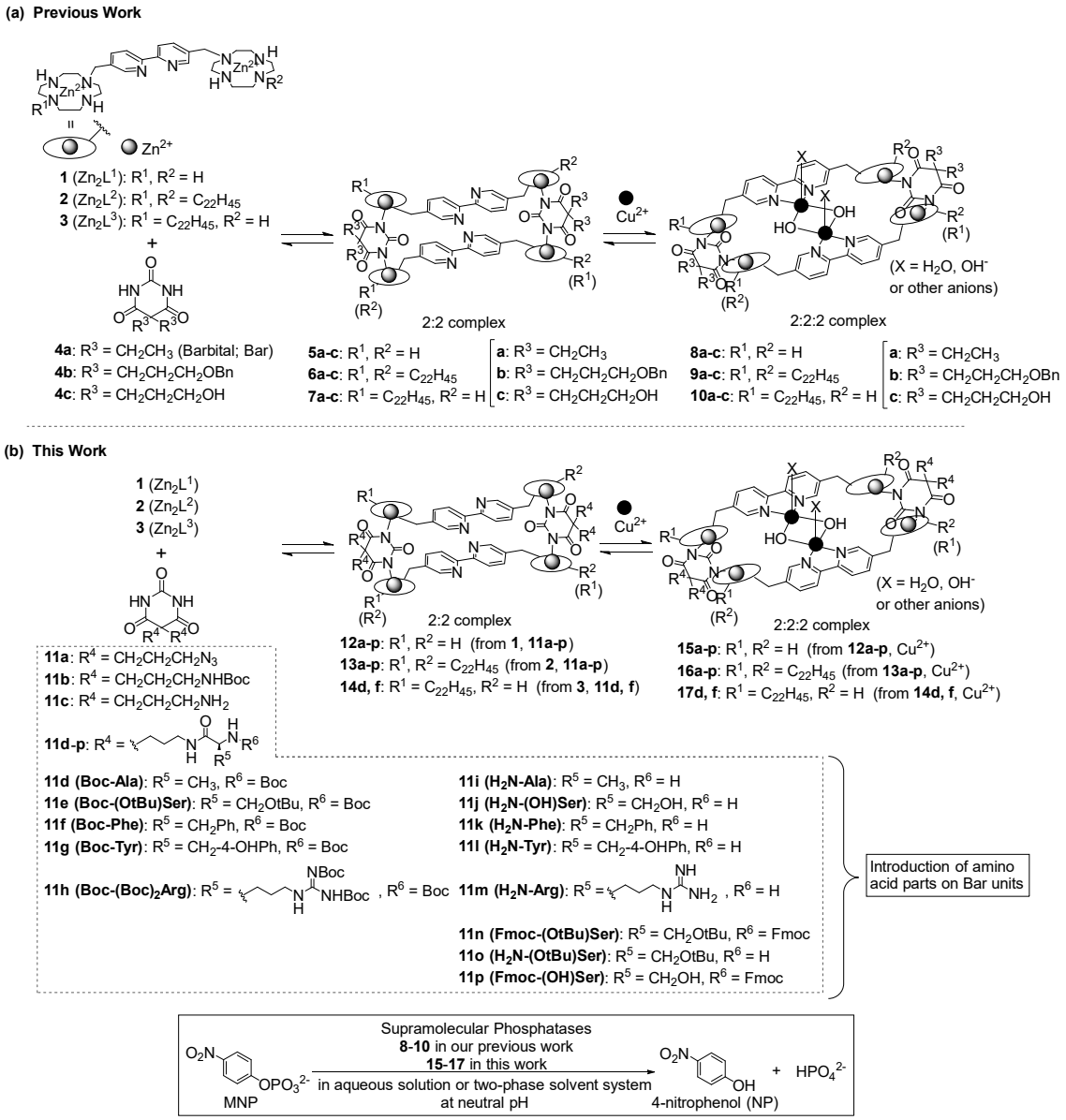

Scheme 1. (**a**) Formation of the 2:2:2 supramolecular complexes **8**–**10** by the self-assembly of Zn_2L complexes (**1**–**3**), 5,5-diethylbarbital (Bar) derivatives (**4a**–**c**) and Cu^{2+} in an aqueous solution at neutral pH or in a two-phase solvent system ($CHCl_3/H_2O$) as was used in our previous study. (**b**) Formation of the 2:2:2 supramolecular complexes **15**–**17** by a self-assembly of Zn_2L complexes (**1**–**3**), 5,5-diethylbarbital (Bar) derivatives (**11a**–**p**) and Cu^{2+} in an aqueous solution at neutral pH or a two-phase solvent system ($CHCl_3/H_2O$) in this work.

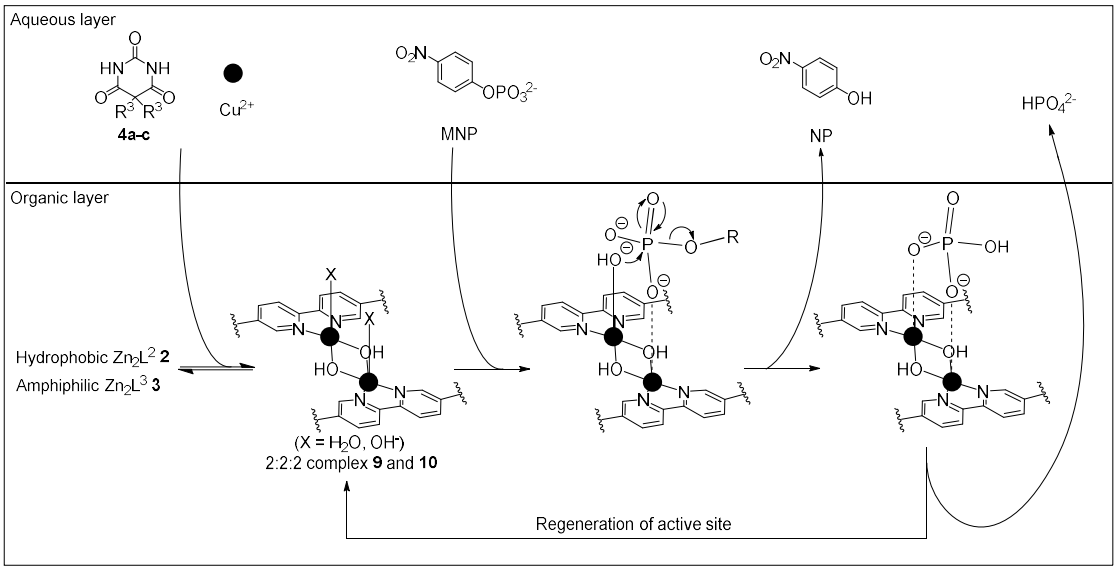

Scheme 2. Concept of the hydrophobic supramolecular complexes **9** and **10** and the hydrolysis of mono(4-nitrophenyl) phosphate (MNP) in a two-phase solvent system, in which the product inhibition by HPO_4^{2-} is avoided.

It is generally accepted that amino acids in the active site of AP contribute to the hydrolysis of phosphomonoesters; for example, the arginine residue captures and fixes the conformation of the phosphomonoester, and the serine residue attacks the phosphorous to promote the hydrolysis [4–10]. These well-grounded assumptions prompted us to introduce amino acids (alanine, serine, arginine, phenylalanine, and tyrosine) into the side chains of the Bar units for the easy and versatile construction of a combinatorial library of supramolecular phosphatases (Scheme 3). For example, functionalization with arginine (Arg) unit would be expected to stabilize the transition state that is produced in the hydrolysis of MNP (Scheme 3a) by electrostatic interactions. Second, the serine (Ser) residue would participate in a nucleophilic attack on the phosphorous of the MNP (Scheme 3b). Third, a phenylalanine (Phe) unit was introduced to support π–π interactions with MNP for a stronger complexation (Scheme 3c). In this paper, we report on the combinatorial construction of 2:2:2 supramolecular complexes **15**–**17** from dinuclear Zn^{2+}-cyclen complexes **1** (Zn_2L^1), **2** (Zn_2L^2), or **3** (Zn_2L^3) with the Bar derivatives that are functionalized with amino acids **11d**–**p** as well as their synthetic intermediates **11a**–**c** and Cu^{2+} (Scheme 1b), their catalytic activity for the hydrolysis of MNP, and the results of a Michaelis–Menten kinetic study. These findings indicate that hydrophobic active sites of the supramolecular phosphatases well mimic the mode of the substrate (MNP) recognition and the product inhibition (by inorganic phosphate), and both of hydrophobic and hydrophilic property of active sites are important for the catalytic turnover of the system.

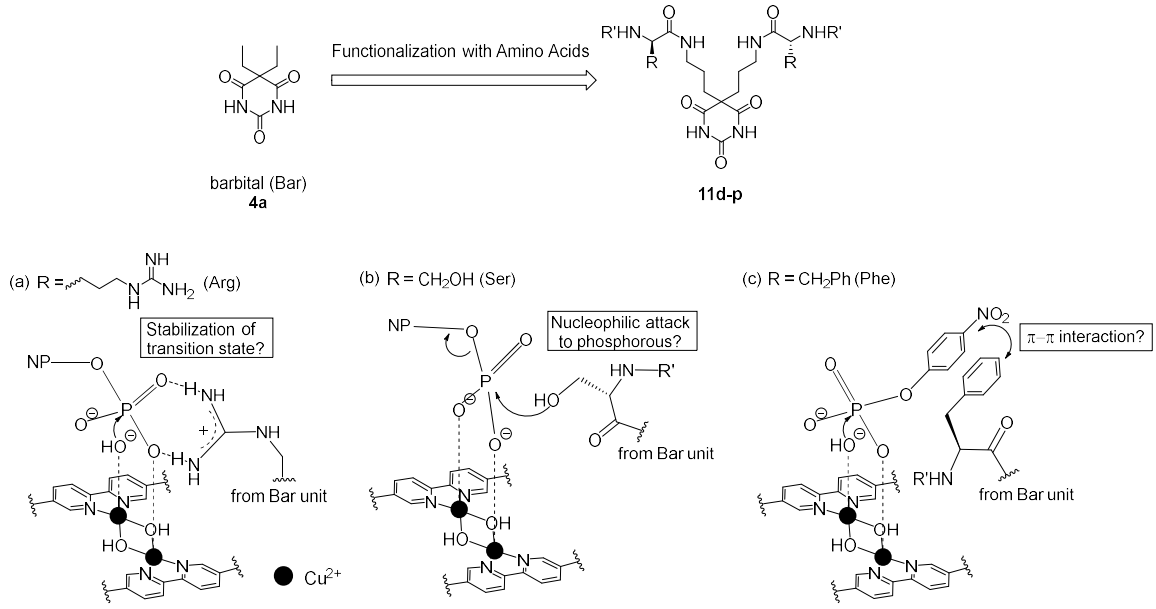

Scheme 3. Predicted effect of new barbital derivatives functionalized with amino acids on the hydrolysis of MNP. (**a**) It is considered that Arg stabilizes the transition state of the MNP hydrolysis by the electrostatic interactions between them, (**b**) Ser is supposed to undergo the nucleophilic attack to the phosphorous of MNP, (**c**) Phe is supposed to contribute to the π–π interactions with MNP.

2. Materials and Methods

2.1. General Information

All reagents and solvents were of the highest commercial quality and were used without further purification, unless otherwise noted. Anhydrous *N*,*N*-dimethylformamide (DMF) was obtained by distillation from calcium hydride. MNP was purchased from Nacalai Tesque (Kyoto, Japan). All aqueous solutions were prepared using deionized and distilled water. The Good's buffer reagents (Dojindo, pK_a at 20 °C) were obtained from commercial sources: HEPES (2-(4-(2-hydroxyethyl)-1-piperazinyl))ethanesulfonic acid, pK_a = 7.6). For the measurement of UV/Vis spectra, $CHCl_3$ was purchased from Nacalai Tesque (Kyoto, Japan). UV/Vis spectra were recorded on a JASCO V-550 spectrophotometer with quartz cuvettes (path length: 10 mm). IR spectra were recorded on a Perkin-Elmer attenuated total reflectance (ATR)-IR spectrometer 100 at room temperature. Melting points were measured on a Yanaco MP-J3 Micro Melting Point apparatus and are uncorrected. ^{1}H- (300 and 400 MHz) and ^{13}C- (75 and 100 MHz) NMR spectra at 25 ± 0.1 °C were recorded on a JEOL Always 300 spectrometer and a JEOL Lamda 400 spectrometer. Tetramethylsilane (TMS) was used as the internal reference for ^{1}H- and ^{13}C-NMR measurements in $CDCl_3$ and CD_3OD. 3-(Trimethylsilyl)propionic-2,2,3,3-d_4 acid sodium salt (TSP) was used as the external reference for ^{1}H- and ^{13}C-NMR measurements in D_2O. Mass spectra was recorded on a JEOL JMS-700 and Varian 910-MS spectrometer. Elemental analyses were performed on a Perkin-Elmer CHN 2400 analyzer. Optical rotations were measured with a JASCO-P-1030 digital polarimeter in 50 mm cells using the D line of sodium (589 nm). Thin-layer chromatography (TLC) and silica gel column chromatography was performed using Merck Silica gel 60 F254 plate or Fuji Silysia Chemical CHROMATOREX NH-TLC PRATE, and Fuji Silysia Chemical FL-100D or Fuji Silysia Chemical CHROMATOREX NH chromatography Silica Gel, respectively.

2.2. Synthesis of Compounds

5,5-Bis[3-(toluenesulfonyl)oxypropyl]barbituric acid (**18**)

A solution of **4c** (698 mg, 2.86 mmol) and DMAP (35 mg, 0.29 mmol) in pyridine (5 mL) was stirred at 0 °C for 5 min, to which *p*-toluenesulfonyl chloride (1.53 g, 8.00 mmol) was slowly added, and the resulting reaction mixture was stirred at room temperature for 2 h. The reaction was quenched by adding an aqueous solution saturated with $NaHCO_3$, and the resulting suspension was extracted with $CHCl_3$ (50 mL × 3). The combined organic layer was washed with brine, dried over Na_2SO_4, and concentrated under reduced pressure. The resulting residue was purified by silica gel column chromatography ($CHCl_3$/MeOH = 1/0 to 50/1) to give **18** as a colorless amorphous solid (819 mg, 54% yield). ^{1}H NMR (300 MHz, $CDCl_3$, TMS): δ = 7.75 (d, J = 8.3 Hz, 4H), 7.35 (d, J = 8.3 Hz, 4H), 3.98–3.92 (m, 4H), 2.45 (s, 6H), 2.12–1.94 (m, 4H), 1.68–1.56 (m, 4H) ppm; ^{13}C NMR (75 MHz, $CDCl_3$, TMS): δ = 171.7, 149.0, 145.1, 132.5, 129.9, 127.9, 69.4, 43.8, 34.0, 24.3, 21.6 ppm; IR (ATR): ν = 3232, 3106, 2962, 2856, 1756, 1696, 1596, 1419, 1346, 1171, 1096, 953, 914, 811, 660, 575, 552, 493. HRMS (ESI): *m/z* calcd for $[M+Na]^+$, $C_{24}H_{28}N_2O_9NaS_2$, 575.1124; found, 575.1129.

5,5-Bis(3-azidopropyl)barbituric acid (**11a**)

A solution of **18** (850 mg, 1.54 mmol) and sodium azide (280 mg, 4.31 mmol) in DMF (4 mL) was stirred at 80 °C for 5 h. After allowing the solution to cool to room temperature, the reaction mixture was poured into H_2O and the resulting mixture was extracted with Et_2O (40 mL × 3). The combined organic layer was washed with brine, dried over Na_2SO_4, and concentrated under reduced pressure. The resulting residue was purified by silica gel column chromatography ($CHCl_3$/MeOH = 1/0 to 10/1) to give **11a** as a white solid (434 mg, 96% yield). ^{1}H NMR (300 MHz, $CDCl_3$, TMS): δ = 8.71 (s, 2H), 3.29 (t, J = 6.6 Hz, 4H), 2.11–2.05 (m, 4H), 1.59–1.49 (m, 4H) ppm; ^{13}C NMR (75 MHz, $CDCl_3$, TMS): δ = 171.5, 55.5, 50.7, 35.6, 24.5 ppm; mp 118–119 °C; IR (ATR): ν = 3198, 3090, 2940, 2862, 2093, 1752, 1694, 1417, 1361, 1326, 1273, 1248, 1199, 1132, 1043, 835, 674, 538, 496. HRMS (ESI): *m/z* calcd for $[M-H]^-$, $C_{10}H_{13}N_8O_3$, 293.1122; found, 293.1116. Anal. Calcd. for $C_{10}H_{14}N_8O_3$: C, 40.82; H, 4.80; N, 38.08; found: C, 40.91; H, 4.74; N, 37.79.

5,5-Bis[3-(*t*-butoxycarbonylamino)propyl]barbituric acid (**11b**)

Solutions of **11a** (420 mg, 1.43 mmol) in AcOEt (2 mL) and Boc_2O (760 mg, 3.48 mmol) in AcOEt (2 mL) were added to a suspension of 10% Pd/C (50 mg) in AcOEt (2 mL) at room temperature under a N_2 atmosphere. The reaction mixture was hydrogenated with H_2 (at 1 atm) at room temperature for 24 h. After the reaction reached completed, the reaction mixture was filtered, and the filtrate was evaporated under reduced pressure. The resulting residue was purified by silica gel column chromatography (AcOEt/Hexanes = 2/3) to give **11b** as a colorless amorphous solid (440 mg, 71% yield). ^{1}H NMR (300 MHz, $CDCl_3$, TMS): δ = 9.32 (brs, 2H), 4.78–4.68 (m, 2H), 3.12–3.00 (m, 4H), 2.01–1.96 (m, 4H), 1.47–1.40 (m, 22H) ppm; ^{13}C NMR (75 MHz, $CDCl_3$, TMS): δ = 172.7, 156.0, 150.0, 79.4, 55.5, 39.9, 35.7, 28.3, 25.4 ppm; IR (ATR): ν = 3357, 3203, 3090, 2977, 2935, 1755, 1686, 1516, 1448, 1392, 1365, 1275, 1248, 1163, 1040, 854, 756, 666, 494. HRMS (ESI): *m/z* calcd for $[M+H]^+$, $C_{20}H_{35}N_4O_7$, 443.2501; found, 443.2500.

5,5-Bis(3-aminopropyl)barbituric acid·2HCl salt (**11c**)

Compound **11b** (440 mg, 0.99 mmol) was dissolved in MeOH (2 mL), to which conc. HCl (2 mL) was added at 0 °C. The mixture was stirred at room temperature for 1 h and concentrated under reduced pressure to give **11c** as a white solid (276 mg, 86% yield as the 2HCl salt). ^{1}H NMR (300 MHz, CD_3OD, TMS): δ = 2.90 (t, J = 7.2 Hz, 4H), 2.05–2.00 (m, 4H), 1.66–1.56 (m, 4H) ppm; ^{13}C NMR (100 MHz, D_2O, TSP): δ = 173.8, 150.5, 55.0, 38.9, 34.2, 22.3 ppm; mp 268 °C; IR (ATR): ν = 2967, 2826, 1749, 1721, 1694, 1591, 1485, 1443, 1397, 1346, 1283, 1220, 981, 819, 492. HRMS (ESI): *m/z* calcd for $[M+H]^+$,

$C_{10}H_{19}N_4O_3$, 243.1456; found, 243.1452. Anal. Calcd. for $C_{10}H_{20}N_4O_3Cl_2$: C, 38.11; H, 6.40; N, 17.78; found: C, 38.31; H, 6.42; N, 17.85.

5,5-Bis{3-[*N*-(*t*-butoxycarbonyl)-L-alanyl]aminopropyl}barbituric acid (**11d**)

To a suspension of **11c** (10 mg, 0.03 mmol) in anhydrous DMF (0.5 mL) and diisopropylethylamine (22 mg, 0.17 mmol), Boc-L-Alanine-OH (13 mg, 0.07 mmol) and PyBOP (36 mg, 0.07 mol) were added and the reaction mixture was stirred at room temperature for 1 h. The reaction mixture was concentrated under reduced pressure, dissolved in $CHCl_3$ (10 mL), washed with a 50% NH_4Cl solution (10 mL × 3), then with brine, dried over Na_2SO_4 and concentrated under reduced pressure. The resulting oil was purified by silica gel column chromatography (AcOEt/Hexanes = 1/2) and reprecipitation with AcOEt and hexanes to give **11d** as a white solid (17 mg, 92% yield). ^{1}H NMR (300 MHz, $CDCl_3$, TMS): δ = 10.2 (brs, 2H), 7.06 (brs, 2H), 5.62–5.58 (m, 2H), 4.22 (brs, 2H), 3.17–3.14 (m, 4H), 1.96–1.92 (m, 4H), 1.45–1.40 (m, 22H), 1.33 (d, J = 5.1 Hz, 6H) ppm; ^{13}C NMR (75 MHz, $CDCl_3$, TMS): δ = 173.5, 172.8, 155.8, 149.9, 55.4, 50.0, 46.3, 39.0, 35.7, 28.4, 24.8, 18.8 ppm; mp 108–109 °C; IR (ATR): ν = 3315, 3092, 2977, 2935, 1754, 1692, 1653, 1522, 1448, 1365, 1246, 1162, 1055, 1021, 856, 759, 495. HRMS (ESI): *m/z* calcd for $[M+H]^+$, $C_{26}H_{45}N_6O_9$, 585.3245; found, 585.3243. Anal. Calcd. for $C_{26}H_{44}N_6O_9 \cdot 0.5H_2O$: C, 52.60; H, 7.64; N, 14.16; found: C, 52.51; H, 7.45; N, 14.20. $[\alpha]^{25}_D$ = −17.9 (c = 1.0, $CHCl_3$).

5,5-Bis{3-[*N*-(*t*-butoxycarbonyl)-*O*-(*t*-butyl)-L-seryl]aminopropyl}barbituric acid (**11e**)

Compound **11e** was synthesized as a white solid (29 mg, 84% yield) from **11c** (10 mg, 0.03 mmol), Boc-L-Serine(OtBu)-OH (18 mg, 0.07 mmol), diisopropylethylamine (22 mg, 0.17 mmol), and PyBOP (36 mg, 0.07 mmol) in anhydrous DMF (0.5 mL) using a procedure similar to that used for **11d**. ^{1}H NMR (300 MHz, $CDCl_3$, TMS): δ = 9.27 (brs, 2H), 6.71 (t, J = 6.0 Hz, 2H), 5.47 (d, J = 6.9 Hz, 2H), 4.20–4.10 (m, 2H), 3.80–3.76 (m, 2H), 3.42–3.36 (m, 2H), 3.30–3.10 (m, 4H), 2.03–1.92 (m, 4H), 1.48–1.39 (m, 22H), 1.18 (s, 18H) ppm; ^{13}C NMR (100 MHz, $CDCl_3$, TMS): δ = 172.2, 171.0, 155.7, 148.8, 80.1, 74.0, 61.8, 55.6, 54.4, 39.0, 35.8, 28.3, 27.4, 25.0 ppm; mp 136–139 °C; IR (ATR): ν = 3332, 3087, 2974, 2934, 2871, 1754, 1697, 1655, 1498, 1390, 1363, 1243, 1163, 1085, 1019, 861, 755, 668, 494. HRMS (ESI): *m/z* calcd for $[M+H]^+$, $C_{34}H_{61}N_6O_{11}$, 729.4387; found, 729.4393. Anal. Calcd. for $C_{34}H_{60}N_6O_{11} \cdot H_2O$: C, 54.68; H, 8.37; N, 11.25; found: C, 54.82; H, 8.43; N, 11.20. $[\alpha]^{25}_D$ = +16.7 (c = 1.0, $CHCl_3$).

5,5-Bis{3-[N-(*t*-butoxycarbonyl)-L-phenylalanyl]aminopropyl}barbituric acid (**11f**)

Compound **11f** was synthesized as a white solid (20 mg, 86% yield) from **11c** (10 mg, 0.03 mmol), Boc-L-Phenylalanine-OH (19 mg, 0.07 mmol), diisopropylethylamine (22 mg, 0.17 mmol), and PyBOP (36 mg, 0.07 mmol) in anhydrous DMF (0.5 mL) using a procedure similar to that used for **11d**. ^{1}H NMR (300 MHz, $CDCl_3$, TMS): δ = 9.43 (brs, 2H), 7.24–7.16 (m, 10H), 6.36–6.26 (m, 2H), 5.32 (d, J = 8.7 Hz, 2H), 4.39–4.30 (m, 2H), 3.20–2.98 (m, 8H), 1.90–1.78 (m, 4H), 1.38 (s, 18H), 1.38–1.24 (m, 4H) ppm; ^{13}C NMR (100 MHz, $CDCl_3$, TMS): δ = 172.5, 171.8, 155.8, 149.5, 136.8, 129.3, 128.5, 126.8, 80.2, 55.9, 55.4, 38.9, 35.5, 28.3, 24.6 ppm; mp 117–118 °C; IR (ATR): ν = 3319, 3088, 2978, 2933, 2859, 1695, 1655, 1526, 1497, 1366, 1249, 1165, 1023, 858, 751, 699, 495. HRMS (ESI): *m/z* calcd for $[M+H]^+$, $C_{38}H_{53}N_6O_9$, 737.3869; found, 737.3869. Anal. Calcd. for $C_{38}H_{52}N_6O_9 \cdot 0.5H_2O$: C, 61.19; H, 7.16; N, 11.27; found: C, 61.18; H, 7.18; N, 11.26. $[\alpha]^{25}_D$ = +2.73 (c = 1.0, $CHCl_3$).

5,5-Bis{3-[*N*-(*t*-butoxycarbonyl)-L-tyrosyl]aminopropyl}barbituric acid (**11g**)

Compound **11g** was synthesized as a white solid (18 mg, 72% yield) from **11c** (10 mg, 0.03 mmol), Boc-L-Tyrosine-OH (20 mg, 0.07 mmol), diisopropylethylamine (22 mg, 0.17 mmol), and PyBOP (36 mg, 0.07 mmol) in anhydrous DMF (0.5 mL) using a procedure similar to that used for **11d**. ^{1}H NMR (300 MHz, CD_3OD, TMS): δ = 7.02 (d, J = 8.7 Hz, 4H), 6.70 (d, J = 8.7 Hz, 4H), 4.18–4.04 (m, 2H), 3.13–3.03 (m, 4H), 2.92 (dd, J = 3.6 Hz, 2H), 2.76–2.64 (m, 2H), 1.88–1.74 (m, 4H), 1.41–1.28 (m, 4H), 1.37 (s, 18H) ppm; ^{13}C NMR (100 MHz, CD_3OD, TMS): δ = 174.5, 157.5, 157.2, 151.2, 131.3, 129.2, 116.2, 80.6, 57.8, 56.5, 40.1, 40.0, 38.8, 37.0, 28.7, 25.8 ppm; mp 150–152 °C; IR (ATR): ν = 3320, 2975, 2930, 1693, 1651,

1515, 1446, 1366, 1244, 1160, 1104, 1019, 829, 779, 494. HRMS (ESI): *m/z* calcd for $[M+H]^+$, $C_{38}H_{53}N_6O_{11}$, 769.3755; found, 769.3767. Anal. Calcd. for $C_{38}H_{52}N_6O_{11}\cdot 2.75H_2O$: C, 55.77; H, 7.08; N, 10.27; found: C, 55.49; H, 6.58; N, 10.80. $[\alpha]^{25}_D$ = +3.63 (*c* = 1.0, CH_3OH).

5,5-Bis{3-[N^{α},N^{ω},N^{δ}-tri(*t*-butoxycarbonyl)-L-arginyl]aminopropyl}barbituric acid (**11h**)

Compound **11h** was synthesized as a white solid (30 mg, 82% yield) from **11c** (10 mg, 0.03 mmol), Boc-L-Arginine(Boc)$_2$-OH (35 mg, 0.07 mmol), diisopropylethylamine (22 mg, 0.17 mmol), and PyBOP (36 mg, 0.07 mmol) in anhydrous DMF (0.5 mL) using a procedure similar to that used for **11d**. ^{1}H NMR (300 MHz, $CDCl_3$, TMS): δ = 9.33 (brs, 2H), 7.14–7.08 (m, 2H), 6.00–5.92 (m, 2H), 4.32–4.22 (m, 2H), 4.04–3.90 (m, 2H), 3.73–3.60 (m, 2H), 3.35–3.05 (m, 4H), 1.94–1.82 (m, 4H), 1.82–1.74 (m, 4H), 1.52 (s, 18H), 1.48 (s, 18H), 1.47–1.30 (m, 12H), 1.44 (s, 18H) ppm; ^{13}C NMR (100 MHz, $CDCl_3$, TMS): δ = 172.3, 171.9, 163.2, 161.0, 155.7, 155.0, 148.5, 84.2, 79.8, 79.4, 55.5, 53.7, 44.0, 39.1, 36.1, 28.9, 28.5, 28.4, 28.1, 25.1, 24.5 ppm; mp 123–125 °C; IR (ATR): ν = 3380, 2977, 2934, 1755, 1709, 1607, 1508, 1452, 1390, 1366, 1271, 1249, 1145, 1099, 981, 886, 852, 811, 779, 512, 496. HRMS (ESI): *m/z* calcd for $[M+H]^+$, $C_{52}H_{91}N_{12}O_{17}$, 1155.6612; found, 1155.6620. Anal. Calcd. for $C_{52}H_{90}N_{12}O_{17}\cdot 0.5H_2O$: C, 53.64; H, 7.88; N, 14.44; found: C, 53.69; H, 8.11; N, 14.21. $[\alpha]^{25}_D$ = +22.3 (*c* = 1.0, $CHCl_3$).

5,5-Bis[3-(L-alanyl)aminopropyl]barbituric acid (**11i**)

Compound **11d** (20 mg, 0.03 mmol) was dissolved in MeOH (0.5 mL), to which conc. HCl (0.5 mL) was added and the reaction mixture was stirred at room temperature for 12 h. The resulting solution was evaporated under reduced pressure to give **11i** as a white solid (16 mg, quant.). ^{1}H NMR (300 MHz, CD_3OD, TMS): δ = 3.88 (q, *J* = 7.2 Hz, 2H), 3.26–3.10 (m, 4H), 1.96–1.91 (m, 4H), 1.49 (d, *J* = 7.2 Hz, 6H), 1.46–1.39 (m, 4H) ppm; ^{13}C NMR (100 MHz, CD_3OD, TMS): δ = 174.6, 170.8, 56.5, 50.3, 40.1, 37.1, 26.1, 18.4, 17.7 ppm; mp 194 °C; IR (ATR): ν = 2933, 1749, 1722, 1666, 1563, 1494, 1447, 1355, 1268, 1206, 1115, 1043, 829, 760, 667, 496. HRMS (ESI): *m/z* calcd for $[M+H]^+$, $C_{16}H_{29}N_6O_5$, 385.2195; found, 385.2194. Anal. Calcd. for $C_{16}H_{28}N_6O_5\cdot 2HCl\cdot H_2O\cdot 1.5MeOH$: C, 40.16; H, 7.32; N, 16.06; found: C, 40.13; H, 7.01; N, 16.09. $[\alpha]^{25}_D$ = +2.24 (*c* = 0.5, CH_3OH).

5,5-Bis[3-(L-seryl)aminopropyl]barbituric acid (**11j**)

Compound **11e** (10 mg, 0.01 mmol) was dissolved in MeOH (0.3 mL), to which conc. HCl (0.3 mL) was added and the reaction mixture was stirred at room temperature for 12 h. The resulting solution was evaporated under reduced pressure to give **11j** as a white solid (7 mg, quant.). ^{1}H NMR (400 MHz, CD_3OD, TMS): δ = 3.95–3.90 (m, 4H), 3.80 (q, *J* = 7.2 Hz, 2H), 3.19 (t, *J* = 7.2 Hz, 4H), 1.96–1.92 (m, 4H), 1.47–1.40 (m, 4H) ppm; ^{13}C NMR (100 MHz, CD_3OD, TMS): δ = 173.2, 166.8, 149.7, 60.4, 55.0, 38.8, 35.6, 33.5, 24.6 ppm; mp 197 °C; IR (ATR): ν = 3197, 3059, 2932, 1748, 1667, 1562, 1495, 1448, 1418, 1356, 1338, 1308, 1272, 1210, 1145, 1045, 761, 498. HRMS (ESI): *m/z* calcd for $[M+H]^+$, $C_{16}H_{29}N_6O_7$, 417.2090; found, 417.2092. Anal. Calcd. for $C_{16}H_{28}N_6O_7\cdot 2HCl\cdot 1.5H_2O\cdot 1.5MeOH$: C, 37.24; H, 6.96; N, 14.89; found: C, 36.96; H, 6.44; N, 14.72. $[\alpha]^{25}_D$ = +5.90 (*c* = 0.5, CH_3OH).

5,5-Bis[3-(L-phenylalanyl)aminopropyl]barbituric acid (**11k**)

Compound **11f** (25 mg, 0.03 mmol) was dissolved in MeOH (0.5 mL), to which conc. HCl (0.5 mL) was added and the reaction mixture was stirred at room temperature for 12 h. The resulting solution was evaporated under reduced pressure to give **11k** as a white solid (22 mg, quant.). ^{1}H NMR (300 MHz, CD_3OD, TMS): δ = 7.35–7.24 (m, 10H), 3.98 (t, *J* = 7.2 Hz, 2H), 3.19–3.13 (m, 2H), 3.10 (d, *J* = 7.2 Hz, 4H), 2.97–2.90 (m, 2H), 1.81 (t, *J* = 8.4 Hz, 4H), 1.23–1.15 (m, 4H) ppm; ^{13}C NMR (100 MHz, CD_3OD, TMS): δ = 174.5, 169.3, 151.2, 135.7, 130.5, 130.1, 128.9, 56.3, 55.9, 40.0, 38.8, 37.1, 25.9 ppm; mp 183–185 °C; IR (ATR): ν = 3189, 3029, 2933, 2818, 1749, 1721, 1668, 1563, 1495, 1454, 1355, 1335, 1303, 1268, 1207, 1144, 1080, 1041, 825, 746, 700, 497. HRMS (ESI): *m/z* calcd for $[M+H]^+$, $C_{28}H_{37}N_6O_5$, 537.2820; found, 537.2820. Anal. Calcd. for $C_{28}H_{36}N_6O_5\cdot 2HCl\cdot 1.5H_2O\cdot MeOH$: C, 52.10; H, 6.78; N, 12.57; found: C, 52.17; H, 6.59; N, 12.64. $[\alpha]^{25}_D$ = +34.9 (*c* = 0.5, CH_3OH).

5,5-Bis[3-(L-tyrosyl)aminopropyl]barbituric acid (**11l**)

A solution of **11g** (25 mg, 0.03 mmol) and conc. HCl (0.5 mL) in MeOH (0.5 mL) was stirred at room temperature for 12 h. The resulting solution was evaporated under reduced pressure to give **11l** as a white solid (21 mg, quant.). ^{1}H NMR (300 MHz, CD_3OD, TMS): δ = 7.04 (d, J = 8.7 Hz, 4H), 6.78 (d, J = 8.7 Hz, 4H), 3.91 (t, J = 7.2 Hz, 2H), 3.16–2.90 (m, 8H), 1.87–1.82 (m, 4H), 1.37–1.31 (m, 4H) ppm; ^{13}C NMR (100 MHz, CD_3OD, TMS): δ = 174.5, 169.7, 158.2, 151.1, 131.6, 126.2, 116.9, 56.5, 56.1, 40.2, 38.0, 37.1, 25.8 ppm; mp 196–198 °C; IR (ATR): ν = 3019, 2934, 1749, 1722, 1668, 1613, 1564, 1514, 1443, 1355, 1306, 1210, 1041, 824, 780, 632, 497. HRMS (ESI): *m/z* calcd for $[M+H]^+$, $C_{28}H_{37}N_6O_7$, 569.2707; found, 569.2718. Anal. Calcd. for $C_{28}H_{36}N_6O_7 \cdot 4HCl \cdot H_2O \cdot MeOH$: C, 45.56; H, 6.06; N, 10.99; found: C, 45.42; H, 5.87; N, 11.13. $[\alpha]^{25}_D$ = +35.6 (c = 1.0, CH_3OH).

5,5-Bis[3-(L-arginyl)aminopropyl]barbituric acid (**11m**)

A solution of **11h** (40 mg, 0.03 mmol) and conc. HCl (0.5 mL) in MeOH (0.5 mL) was stirred at room temperature for 12 h. The resulting solution was evaporated under reduced pressure to give **11m** as a white solid (22 mg, quant.). ^{1}H NMR (300 MHz, CD_3OD, TMS): δ = 3.89 (t, J = 6.0 Hz, 2H), 3.30–3.26 (m, 8H), 3.18–3.09 (m, 2H), 1.98–1.87 (m, 8H), 1.74–1.67 (m, 4H), 1.45–1.43 (m, 4H) ppm; ^{13}C NMR (100 MHz, CD_3OD, TMS): δ = 174.6, 169.9, 158.7, 151.0, 56.5, 54.1, 41.9, 40.2, 37.2, 29.8, 26.0, 25.6 ppm; mp 182–184 °C; IR (ATR): ν = 3157, 3058, 2936, 1749, 1722, 1655, 1561, 1498, 1446, 1355, 1303, 1270, 1209, 1162, 1042, 827, 663, 496. HRMS (ESI): *m/z* calcd for $[M+H]^+$, $C_{22}H_{43}N_{12}O_5$, 555.3480; found, 555.3474. Anal. Calcd. for $C_{22}H_{42}N_{12}O_5 \cdot 4HCl \cdot 2H_2O \cdot MeOH$: C, 35.94; H, 7.08; N, 21.87; found: C, 35.87; H, 6.89; N, 21.83. $[\alpha]^{25}_D$ = +10.7 (c = 1.0, CH_3OH).

5,5-Bis{3-[*N*-(9-fluorenylmethoxycarbonyl)-*O*-(*t*-butyl)-L-seryl]aminopropyl}barbituric acid (**11n**)

Compound **11n** was synthesized as a white solid (31 mg, 98% yield) from **11c** (10 mg, 0.03 mmol), Fmoc-L-Serine(OtBu)-OH (27 mg, 0.07 mmol), diisopropylethylamine (22 mg, 0.17 mmol), and PyBOP (36 mg, 0.07 mmol) in anhydrous DMF (0.5 mL) using a procedure similar to that used for **11d**. ^{1}H NMR (300 MHz, $CDCl_3$, TMS): δ = 9.03 (brs, 2H), 7.75 (d, J = 7.2 Hz, 4H), 7.62–7.54 (m, 4H), 7.39 (t, J = 7.2 Hz, 4H), 7.29 (t, J = 7.2 Hz, 4H), 6.70–6.58 (m, 2H), 5.80 (d, J = 7.2 Hz, 2H), 4.40 (d, J = 6.9 Hz, 4H), 4.21 (t, J = 7.2 Hz, 4H), 3.76 (dd, J = 3.9 Hz, 2H), 3.38 (t, J = 8.1 Hz, 2H), 3.28–3.10 (m, 4H), 2.02–1.88 (m, 4H), 1.50–1.36 (m, 4H), 1.17 (s, 18H) ppm; ^{13}C NMR (100 MHz, $CDCl_3$, TMS): δ = 172.0, 170.5, 156.2, 148.6, 143.8, 141.3, 127.7, 127.1, 125.2, 120.0, 74.2, 67.1, 61.7, 55.6, 54.6, 47.1, 39.0, 35.7, 27.4, 24.9 ppm; mp 122–124 °C; IR (ATR): ν = 3313, 3064, 2972, 2934, 2870, 1698, 1659, 1516, 1449, 1410, 1389, 1363, 1330, 1235, 1191, 1081, 1023, 874, 758, 738, 664, 620, 539, 496. HRMS (ESI): *m/z* calcd for $[M+H]^+$, $C_{54}H_{65}N_6O_{11}$, 973.4707; found, 973.4706. Anal. Calcd. for $C_{54}H_{64}N_6O_{11} \cdot H_2O$: C, 65.44; H, 6.71; N, 8.48; found: C, 65.23; H, 6.77; N, 8.30. $[\alpha]^{25}_D$ = +20.4 (c = 1.0, $CHCl_3$).

5,5-Bis{3-[*O*-(*t*-butyl)-L-seryl]aminopropyl}barbituric acid (**11o**)

To a solution of **11n** (15 mg, 0.02 mmol) in anhydrous DMF (0.4 mL), piperidine (0.1 mL) was added and the reaction mixture was stirred at room temperature for 20 min. The reaction mixture was concentrated under reduced pressure, and resulting residue was purified by silica gel column chromatography (AcOEt/MeOH = 1/0 to 6/1) to give **11o** as a colorless amorphous solid (7 mg, 92% yield). ^{1}H NMR (400 MHz, $CDCl_3$, TMS): δ = 7.53–7.48 (m, 2H), 3.62 (q, J = 4.0 Hz, 2H), 3.53 (q, J = 4.0 Hz, 2H), 3.44 (t, J = 8.0 Hz, 2H), 3.24–3.14 (m, 4H), 1.98–1.90 (m, 4H), 1.50–1.36 (m, 4H), 1.18 (s, 18H) ppm; ^{13}C NMR (100 MHz, $CDCl_3$, TMS): δ = 173.2, 173.0, 150.2, 73.6, 64.0, 55.6, 55.5, 38.8, 35.9, 27.6, 25.1 ppm; IR (ATR): ν = 3299, 3072, 2971, 2928, 2856, 1723, 1693, 1646, 1533, 1448, 1411, 1388, 1362, 1335, 1306, 1258, 1192, 1078, 1022, 874, 759, 670, 493. HRMS (ESI): *m/z* calcd for $[M+H]^+$, $C_{24}H_{45}N_6O_7$, 529.3344; found, 529.3344. $[\alpha]^{25}_D$ = −14.5 (c = 1.4, $CHCl_3$).

5,5-Bis{3-[*N*-(9-fluorenylmethoxycarbonyl)-L-seryl]aminopropyl}barbituric acid (**11p**)

To a solution of **11n** (11 mg, 0.01 mmol) in dichloromethane (0.2 mL), trifluoroacetic acid (0.2 mL) was added and the reaction mixture was stirred at room temperature for 2 h. The reaction mixture was concentrated under reduced pressure, suspended in H_2O, extracted with AcOEt (10 mL × 3), washed with brine, dried over Na_2SO_4, and concentrated under reduced pressure. The resulting residue was purified by silica gel column chromatography (AcOEt/Hexanes = 4/1 to 1/0) to give **11p** as a white solid (5 mg, 54% yield). ^{1}H NMR (400 MHz, CD_3OD, TMS): δ = 7.78 (d, J = 7.6 Hz, 4H), 7.67 (t, J = 7.6 Hz, 4H), 7.38 (t, J = 7.6 Hz, 4H), 7.30 (t, J = 7.6 Hz, 4H), 4.39 (dd, J = 2.4 Hz, 4H), 4.23 (t, J = 6.8 Hz, 2H), 4.12 (t, J = 6.8 Hz, 2H), 3.72 (d, J = 5.2 Hz, 4H), 3.17–3.08 (m, 4H), 1.96–1.84 (m, 4H), 1.43–1.34 (m, 4H) ppm; ^{13}C NMR (100 MHz, CD_3OD, TMS): δ = 174.6, 172.9, 158.5, 151.0, 145.4, 145.3, 142.6, 128.8, 128.2, 126.3, 121.0, 68.1, 63.3, 58.7, 56.5, 40.0, 36.9, 25.9 ppm; mp 124–125 °C; IR (ATR): ν = 3316, 3067, 2932, 2854, 1695, 1657, 1528, 1448, 1415, 1334, 1245, 1203, 1137, 1060, 758, 738, 620, 538, 498. HRMS (ESI): *m/z* calcd for $[M+Na]^+$, $C_{46}H_{48}N_6O_{11}Na$, 883.3283; found, 883.3273. Anal. Calcd. for $C_{46}H_{48}N_6O_{11}\cdot 2H_2O$: C, 61.60; H, 5.84; N, 9.37; found: C, 61.77; H, 5.69; N, 8.98. $[\alpha]^{25}_D$ = −9.50 (c = 0.7, CH_3OH).

2.3. Hydrolysis of MNP

The hydrolysis of MNP was carried out in 10 mM HEPES buffer (pH 7.4) with I = 0.1 ($NaNO_3$) (for **8, 15**) and in a $CHCl_3$/50 mM HEPES buffer (pH 7.4) with I = 0.1 ($NaNO_3$) (2/8) (for **9**, **10**, **16**, **17**) at 37 °C. Stock solutions of **1** (3.0 mM in H_2O), **4** or **11** (6.0 mM in H_2O), and $CuNO_3\cdot 3H_2O$ (10 mM in H_2O) were used for the preparation of sample solutions of **8** and **15** (20 μM) in 10 mM HEPES buffer (pH 7.4) with I = 0.1 ($NaNO_3$) (3.0 mL). Stock solutions of **2** (1.0 mM in $CHCl_3$), **4** or **11** (3.0 mM in H_2O or $CHCl_3$), and $Cu(ClO_4)_2\cdot 6H_2O$ (20 mM in H_2O) were used for the preparation of sample solutions of **9** and **16** (20 μM in total solution) in $CHCl_3$/50 mM HEPES buffer (pH 7.4) with I = 0.1 ($NaNO_3$) (2/8) (total volume 3.0 mL). A stock aqueous solution of MNP (20 mM) was used for the hydrolysis reaction. Prior to the hydrolysis of MNP in the two-phase solvent system, the reaction mixtures of **2** or **3**, barbital derivatives (**4a–c**, **11a–p**), and Cu^{2+} in $CHCl_3$/50 mM HEPES buffer (pH 7.4) with I = 0.1 ($NaNO_3$) (2/8) were incubated at 37 °C overnight using a shaking water bath (shaking speed: 150 rpm) (Tokyo Glass Kikai, FWB-1) to form **9**, **10**, **16**, and **17** *in situ*, and the aqueous solution of MNP was added. All of the hydrolysis experiments were performed in triplicate at 37 °C using a shaking water bath (shaking speed: 150 rpm). The yields of the hydrolysis product from MNP in the presence of the supramolecular complexes were calculated based on the increase in the absorption of the released 4-nitrophenol (NP) at 400 nm ([NP produced in the presence of the supramolecular complex]–[NP produced in the absence of the supramolecular complex]) (ε_{400} value of NP is 1.35×10^4 $M^{-1}\cdot cm^{-1}$ at pH 7.4) [17] in aqueous layer. The partition ratio of NP (79% in aqueous solution), which had been determined in the previous report [53], was used for the calculation of the yields in the $CHCl_3/H_2O$ system.

3. Results and Discussion

3.1. Synthesis of Barbital Derivatives

The barbital derivatives that were functionalized with amino acid residues were synthesized as shown in Scheme 4. Compound **4c** was synthesized from diethyl malonate via **4b** according to our previous paper [24] and was reacted with *p*-toluenesulfonyl chrolide to afford the ditosylate **18**. The reaction of **18** with sodium azide gave compound **11a**. Our attempt to carry out Staudinger reactions [55,56] of **11a** with the *o*-phosphynothioesters of amino acids resulted in failure. Therefore, the reduction of the azide groups of **11a** were carried out to obtain the diamino intermediate **11c**. It should be noted that two amino groups of **11c** produced by the reduction of **11a** were directly protected with a Boc group *in situ* for easy purification as a Boc-protected compound **11b** and the subsequent deprotection of the Boc groups afforded **11c**. The condensation reactions of **11c** with Boc-protected amino acids in DMF in the presence of PyBOP and DIEA gave **11d–h**. The deprotection of the Boc groups by treatment with HCl afforded the corresponding compounds **11i–m** in quantitative yield.

The barbital derivative equipped with serine **11n** was obtained from **11c** and Fmoc-L-Ser(OtBu)-OH and then reacted with piperidine and TFA to give compound **11o** and **11p**, respectively.

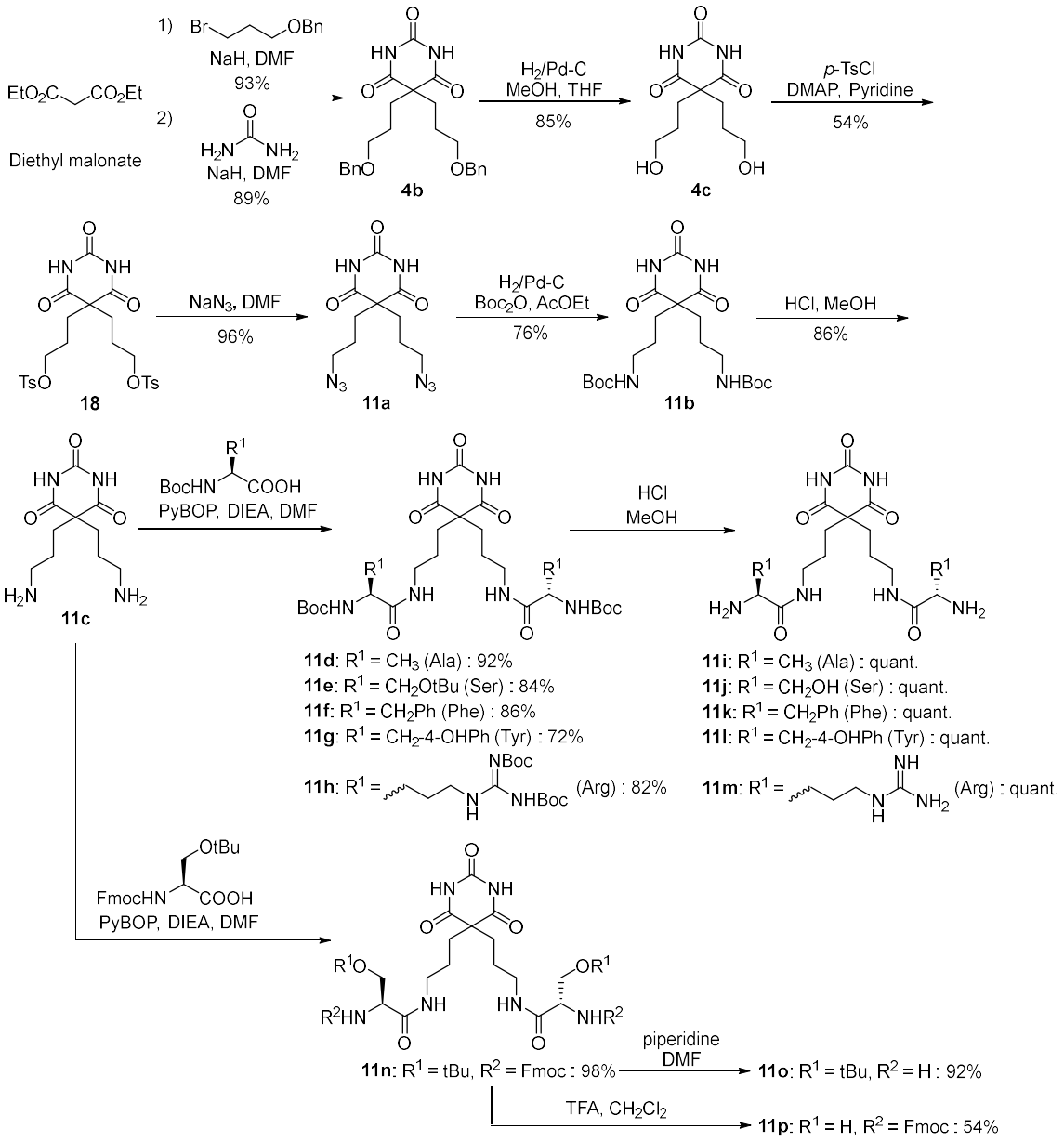

Scheme 4. Synthesis of barbital derivatives **11a**–**p** as building units for supramolecular complexes **15**, **16** and **17**.

3.2. Complexation Behavior of 1 (Zn_2L^1) with Barbital Derivatives and Cu^{2+} by UV/Vis Titrations

In order to examine the formation of the 2:2 and 2:2:2 supramolecular complexes from the bis(Zn^{2+}-cyclen) complexes **1** (Zn_2L^1) and **2** (Zn_2L^2) with the synthesized Bar units and Cu^{2+} as shown in Scheme 1, UV/Vis titrations of the bis(Zn^{2+}-cyclen) complexes with **11d** and **11i**, and then with $Cu(NO_3)_2{\cdot}3H_2O$ were attempted. While the titrations of **2** in the two-phase solvent system ($CHCl_3$/50 mM HEPES buffer (pH 7.4, I = 0.1 ($NaNO_3$)) with **11d** and **11i** and $Cu(ClO_4)_2{\cdot}6H_2O$ were unsuccessful, the UV/Vis titrations of **1** with **11d** and **11i** were successfully carried out in 10 mM HEPES buffer (pH 7.4, I = 0.1 ($NaNO_3$)) at 37 °C. As shown in Figure 1a,b, 80 μM of **1** has an absorption maxima (λ_{max}) at 287 nm, which increased upon the addition of **11d** and decreased upon the addition of **11i**, reaching a plateau at a 1:1 ratio, suggesting a 2:2 assembly of **1** with **11d** or **11i** as same as that with **4a**. In

addition, as shown in Figure 1c,d, the addition of Cu^{2+} induced a red shift from 287 nm to 309 nm, which reached a plateau at [**12d**] (or [**12i**]):[Cu^{2+}] = 1:2, suggesting the quantitative formation of the 2:2:2 supermolecules **15** with newly synthesized barbital derivatives at μM order concentrations.

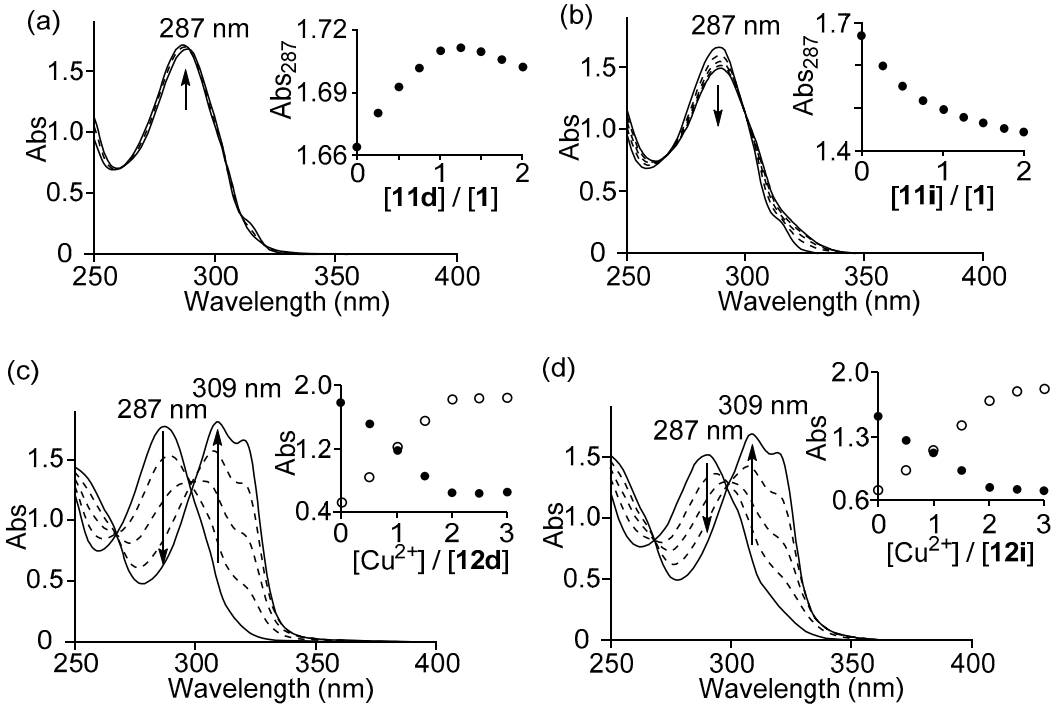

Figure 1. (**a**) UV/Vis titration of **1** (80 μM) upon the addition of **11d** in 10 mM HEPES buffer (pH 7.4 with I = 0.1 ($NaNO_3$)) at 25 °C; (**b**) UV/Vis titration of **1** (80 μM) upon the addition of **11i** in 10 mM HEPES buffer (pH 7.4 with I = 0.1 ($NaNO_3$)) at 25 °C; (**c**) UV/Vis titration of **12d** (40 μM) upon the addition of Cu^{2+} in 10 mM HEPES buffer (pH 7.4 with I = 0.1 ($NaNO_3$)) at 25 °C; (**d**) UV/Vis titration of **12i** (40 μM) upon the addition of Cu^{2+} in 10 mM HEPES buffer (pH 7.4 with I = 0.1 ($NaNO_3$)) at 25 °C. The insets in (**a**,**b**) show the change in the absorbance at 287 nm, and the insets in (**c**,**d**) show the decrease in absorbance at 287 nm (closed circles) and the increase in absorbance at 309 nm (open circles).

3.3. Location of Complexes 13 and 16 in the Two-Phase Solvent System, as Determined by UV/Vis Spectra

The distribution of **13** and **16** in the organic phase and the aqueous phase of the two-phase solvent system was determined from the UV/Vis absorption spectra of both layers, as described in our previous report [54]. For the *in situ* formation of **13** and **16**, **11d** and **11f** were selected as more hydrophobic barbital units, and **4a**, **11i,** and **11k** were selected as more hydrophilic barbital units. Two-phase solutions of Zn_2L^2 (**2**) alone (40 μM), 2:2 complex (20 μM) of Zn_2L^2 and barbital derivatives (**6a**, **13d**, **13f**, **13i**, and **13k**), and 2:2:2 complex (20 μM) of Zn_2L^2, barbital derivatives, and Cu^{2+} (**9a**, **16d**, **16f**, **16i**, and **16k**) were prepared in $CHCl_3$/50 mM HEPES buffer (pH 7.4) with I = 0.1 ($NaNO_3$) (1/1), incubated for 18 h at 37 °C, and centrifuged (2000 rpm × 10 min) at room temperature. Pictures of each complex and their distribution ratios are summarized in Figure 2 and Table 1. The findings indicate that **2** is located mostly in the organic layer (*ca.* 99%), and the addition of barbital derivatives did not significantly affect the distribution of **6a**, **13d**, **13f**, **13i**, and **13k** (*ca.* 96%–>99%), implying that these complexes are distributed mainly in the organic layer. Since the addition of Cu^{2+} quenched the emission from the bpy units, it was not possible to determine the distribution of **9a**, **16d**, **16f**, **16i**, and **16k** in both layers. These behaviors of **6a**, **13d**, **13f**, **13i**, and **13k** are different from **7a** prepared from **3** (Zn_2L^3) and **4a** (Bar), which were distributed both in the aqueous and the organic layers [54].

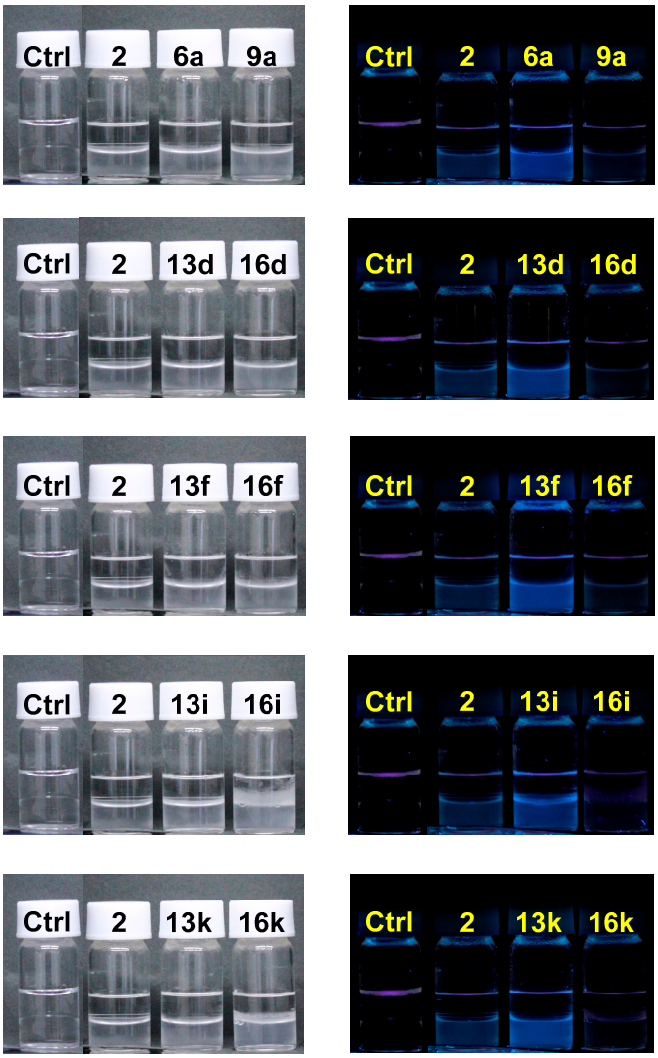

Figure 2. Photos of mixtures of **2** (Zn_2L^2), the complexes of **2** with barbital derivatives (**4a**, **11d**, **11f**, **11i**, and **11k**) (**6a**, **13d**, **13f**, **13i**, and **13k**), and the 2:2:2 complexes of **2**, Bar units and Cu^{2+} (**9a**, **16d**, **16f**, **16i**, and **16k**) in $CHCl_3$/50 mM HEPES buffer (pH 7.4) with I = 0.1 ($NaNO_3$) (1/1) at room temperature.

Table 1. Distribution of each complex ([**6a**, **13**] = 20 μM in the total solvent including both the aqueous and the $CHCl_3$ phase) in the aqueous layer and the organic layer, as estimated by UV/Vis absorption spectra of these complexes in each layer.

-	In H_2O Layer (%)	In $CHCl_3$ Layer (%)
5a [a]	>98	<2
6a	1	99
7a [a]	35	65
13d	2	98
13f	4	96
13i	<1	>99
13k	<1	>99

[a] From ref. 54 ([**5a** and **7a**] = 50 μM in total solvent including aqueous and $CHCl_3$ phase).

3.4. Hydrolysis of MNP by 2:2:2 Complexes in a Two-Phase Solvent System

We conducted the hydrolysis of MNP (100 μM) in the single-phase solvent system (10 mM HEPES buffer (pH 7.4) with I = 0.1 ($NaNO_3$)) at 37 °C in the presence of **8a** or **15i–m** (prepared from **1**, **11i–m**,

and Cu^{2+}) (100 μM) [24] and in the two-phase solvent system ($CHCl_3$/50 mM HEPES buffer (pH 7.4) with I = 0.1 ($NaNO_3$)) (2/8) at 37 °C in the presence of **9a** or **16i**–**m** (prepared from **2**, **11i**–**m**, and Cu^{2+}) (20 μM in the total solution including the aqueous phase and the $CHCl_3$ phase). The results showed that the MNP hydrolysis in the presence of **15i**–**m** was much slower than that of **8a** in the single-phase solvent system, as shown in Figure 3.

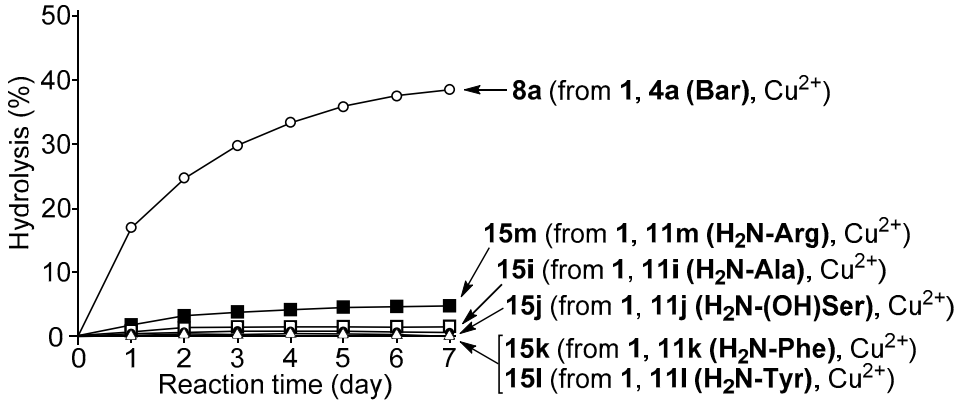

Figure 3. Hydrolysis of MNP (100 μM in the total solution) by **8a** (open circles), **15i** (open squares), **15j** (closed circles), **15k** (open triangles), **15l** (open triangles), or **15m** (closed squares) ([**8** or **15**] = 100 μM) in a single aqueous phase (10 mM HEPES buffer (pH 7.4) with I = 0.1 ($NaNO_3$)) at 37 °C.

As shown in Figure 4a, the activity of **16i**–**m** (20 μM) was similar to that of **9a** in the two-phase solvent system with negligible catalytic turnover (note that [**16i**–**m**] = 20 μM), suggesting that more hydrophobic supermolecules have higher hydrolysis activity in the two-phase solvent system than in the single-phase solvent system. Interestingly, the MNP hydrolysis activity for **16d**–**h** (prepared from **2**, **11d**–**h**, and Cu^{2+}) was higher than that of **16i**–**m** under the same conditions, as shown in Figure 4b, and the hydrolysis yields for **16d** and **16f** were in excess of 20% after 1 day and in excess of 25%–40% after 7 days, indicating that these complexes had catalytic activities. Moreover, the activities of **16a** and **16b** were similar to that for **16d**–**h** (Figure 5), suggesting that the azide and Boc-protected amino groups on the Bar unit provide a similar effect on the hydrolysis of MNP as those of the protected amino acid residues in **16d**–**g**.

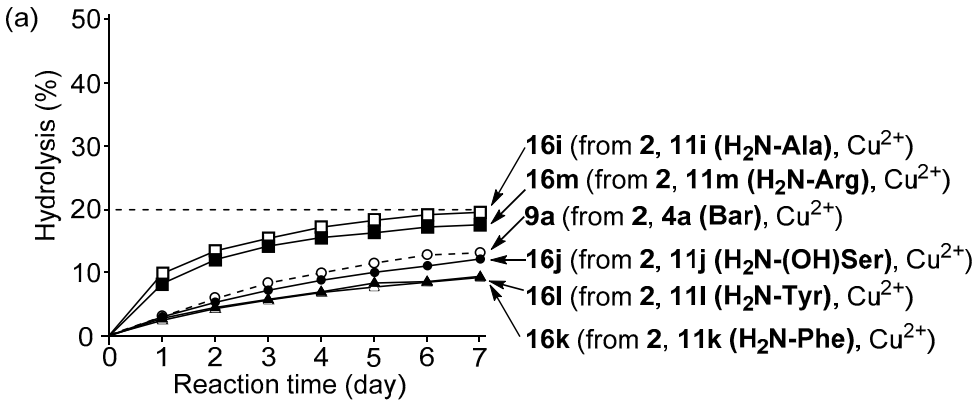

Figure 4. *Cont.*

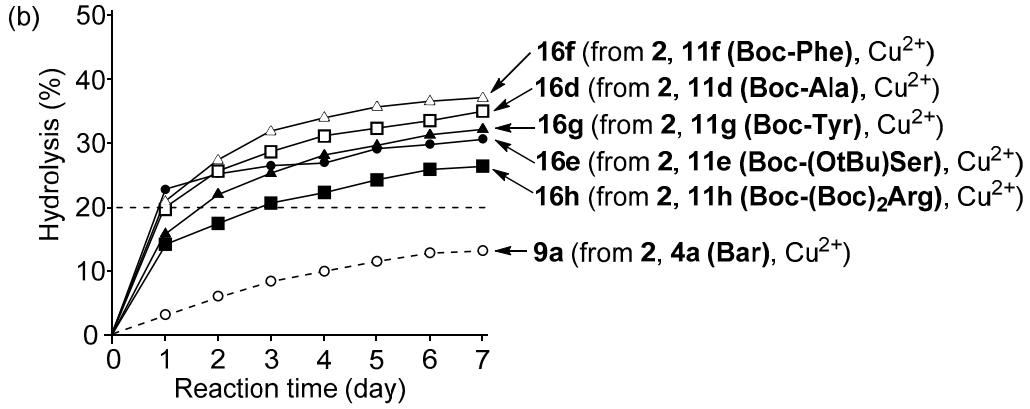

Figure 4. Hydrolysis of MNP (100 μM in the total solution) by (**a**) **9a** (open circles with dashed curve), **16i** (open squares), **16j** (closed circles), **16k** (open triangles), **16l** (closed triangles), or **16m** (closed squares) ([**9**, **16**] = 20 μM in the total solution); (**b**) **9a** (open circles with dashed curve), **16d** (open squares), **16e** (closed circles), **16f** (open triangles), **16g** (closed triangles), or **16h** (closed squares) ([**9**, **16**] = 20 μM in the total solution) in $CHCl_3$/50 mM HEPES buffer (pH 7.4) with I = 0.1 ($NaNO_3$) (2/8) at 37 °C. The concentrations of the product (4-nitrophenol) were determined in the total two-phase solvent system.

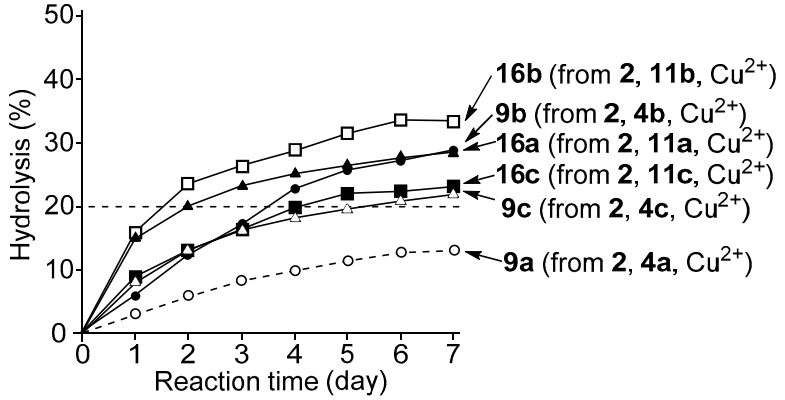

Figure 5. Hydrolysis of MNP (100 μM in the total solution) by **9a** (open circles), **9b** (closed triangles), **9c** (open triangles), **16a** (closed circles), **16b** (open squares), and **16c** (closed squares) ([**9**, **16**] = 20 μM in the total solution) in $CHCl_3$/50 mM HEPES buffer (pH 7.4) with I = 0.1 ($NaNO_3$) (2/8) at 37 °C. The concentrations of the product (4-nitrophenol) were determined in the total two-phase solvent system.

Figure 6 summarizes the results for the hydrolysis of MNP by **16e**, **16j**, **16n**, **16o**, and **16p**, which contain serine units ([MNP] = 100 μM and [**16e**, **16j**, **16n**, **16o**, and **16p**] = 20 μM). The findings suggest that **16e** and **16n** consisting of the fully protected Ser have a higher activity than **16j**, **16o**, and **16p** in which the Bar units contain fully or partially deprotected Ser.

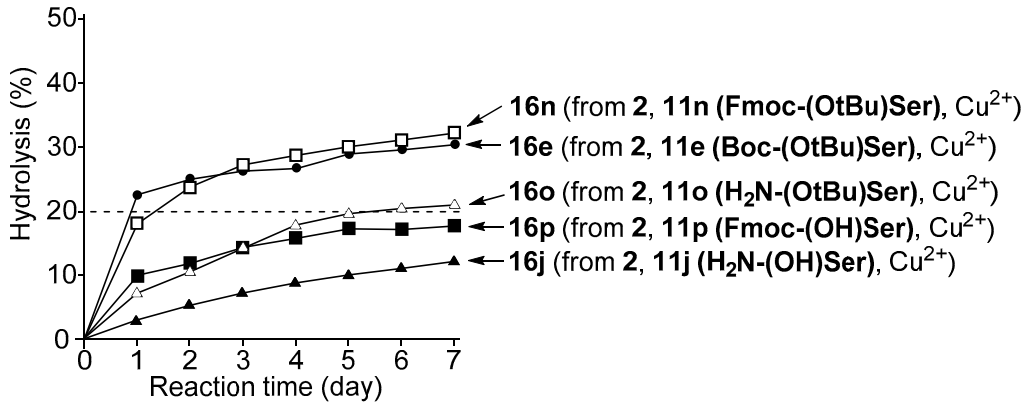

Figure 6. Hydrolysis of MNP (100 μM in the total solution) by **16e** (closed circles), **16j** (closed triangles), **16n** (open squares), **16o** (open triangles), and **16p** (closed squares) (barbital derivatives containing serine residue) ([**16**] = 20 μM in the total solution) in $CHCl_3$/50 mM HEPES buffer (pH 7.4) with I = 0.1 ($NaNO_3$) (2/8) at 37 °C. The concentrations of the product (4-nitrophenol) were determined in the total solution of the two-phase solvent system.

The hydrolysis of MNP (100 μM) by the amphiphilic supramolecular complexes **17d** or **17f** (prepared from **3**, **11d,** or **11f**, and Cu^{2+}) (20 μM) was also examined. As shown in Figure 7, the hydrolytic activity of **17d** and **17f** were higher than **9a**, but slightly lower than **16d** and **16f**.

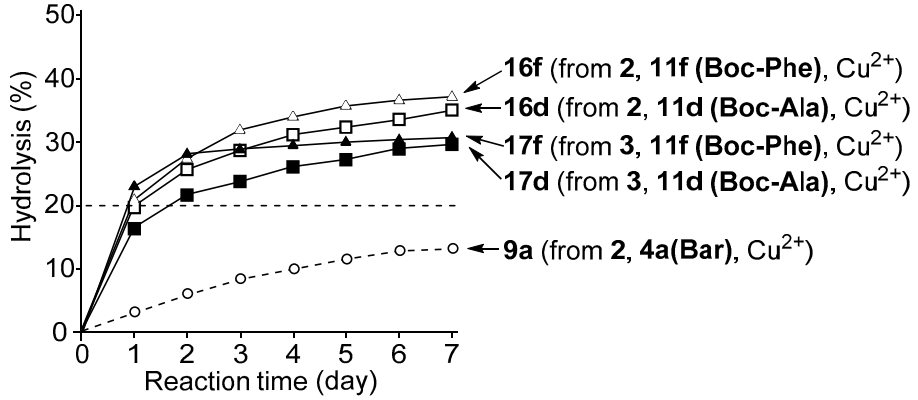

Figure 7. Hydrolysis of MNP (100 μM in the total solution) by **9a** (open circles), **16d** (open squares), **16f** (open triangles), **17d** (closed squares), and **17f** (closed triangles) ([**9**, **16**, **17**] = 20 μM in the total solution) in $CHCl_3$/50 mM HEPES buffer (pH 7.4) with I = 0.1 ($NaNO_3$) (2/8) at 37 °C. The concentrations of the product (4-nitrophenol) were determined in the total two-phase solvent system.

The hydrolysis of MNP by **16d**–**m**, **17d** and **17f** (20 μM) was carried out at higher concentrations of MNP (200, 300, 400, 500, and 1000 μM) and the typical results at [MNP] = 1000 μM are summarized in Figure 8 (the results for **9a** are included in all of the graphs as standard data), in which **16d**–**g** formed from the *N*-protected barbital units **11d**–**g** showed higher hydrolysis activities. It should be noted that **16f** demonstrated the highest MNP hydrolysis yield as shown in Figure 8b, and the catalytic turnover number (CTN) was more than 2 after 1 day. The CTN values for **9a**, **10a**, **16b**, **16d**–**n**, **17d**, and **17f** at [MNP] =1000 μM, which are summarized in Figure 9, imply that the CTNs of **16b**, **16e**, **16f**, **16g**, **17d**, and **17f** are over 2, while these values are smaller than that of our previously reported **10a** (~4) [54].

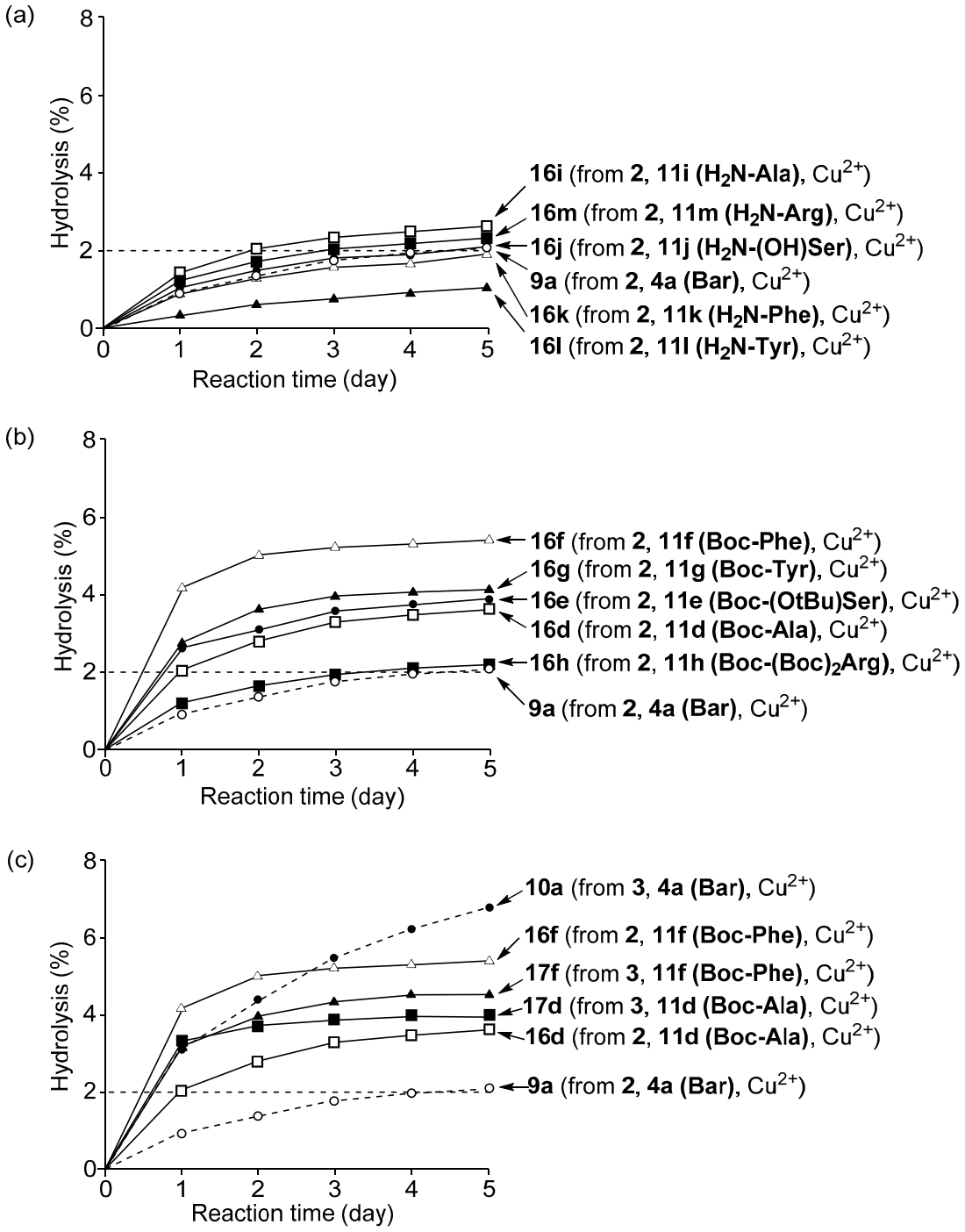

Figure 8. Hydrolysis of MNP (1000 μM in the total solution) by (**a**) **9a** (open circles with dashed curve), **16i** (open squares), **16j** (closed circles), **16k** (open triangles), **16l** (closed triangles), or **16m** (closed squares); (**b**) The hydrolysis of MNP by **9a** (open circles with dashed curve), **16d** (open squares), **16e** (closed circles), **16f** (open triangles), **16g** (closed triangles), or **16h** (closed squares); (**c**) The hydrolysis of MNP by **9a** (open circles with dashed curve), **10a** (closed circles with dashed curve), **16d** (open squares), **16f** (open triangles), **17d** (closed squares), **17f** (closed triangles) ([**9**, **16**, **17**] = 20 μM in the total solution) in $CHCl_3$/50 mM HEPES buffer (pH 7.4) with I = 0.1 ($NaNO_3$) (2/8) at 37 °C. The concentrations of the product (4-nitrophenol) were determined in the total two-phase system.

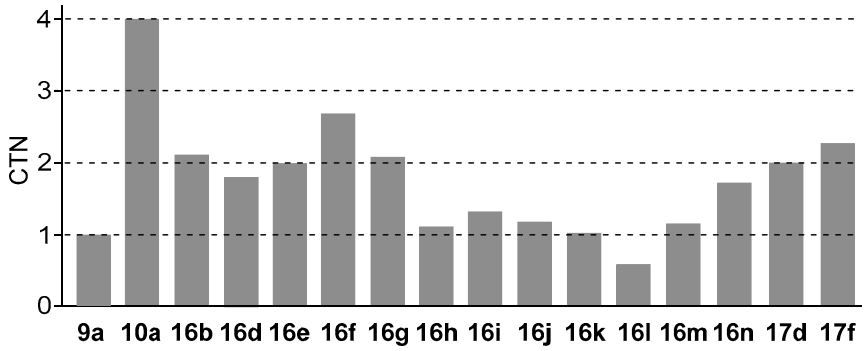

Figure 9. Comparison of catalytic turnover numbers (CTN) of **9a**, **10a**, **16b**, **16d**–**n**, **17d**, and **17f** at [MNP] = 1000 μM and [**9**, **16**, **17**] = 20 μM (in the total solution) in $CHCl_3$/50 mM HEPES buffer (pH 7.4) with I = 0.1 ($NaNO_3$) (2/8) at 37 °C.

3.5. Michaelis–Menten Kinetics for Hydrolysis of MNP by 9, 16, and 17 in the Two-Phase Solvent System

The results for the hydrolysis of MNP by the supramolecular phosphatases at [MNP] = 100, 200, 500, 800, and 1000 μM (in the total solution) were analyzed based on Michaelis–Menten kinetics, as described in our previous reports (the hydrolysis of MNP by **16d**, **16h**, and **16i** were carried out at [MNP] = 100, 200, 300, 400, and 500 μM (in the total solution)) [19,24,53,54]. Based on the Lineweaver–Burk plots shown in Figure 10, V_{max} (the maximum velocity for the formation of NP from MNP promoted by **9**, **16**, and **17**, μM min^{-1}), K_m (Michaelis constant, μM), and k (the first-order rate constant defined by Equation (1), min^{-1}) [57] values were determined and summarized in Table 2.

$$k = V_{max}/K_m \quad (1)$$

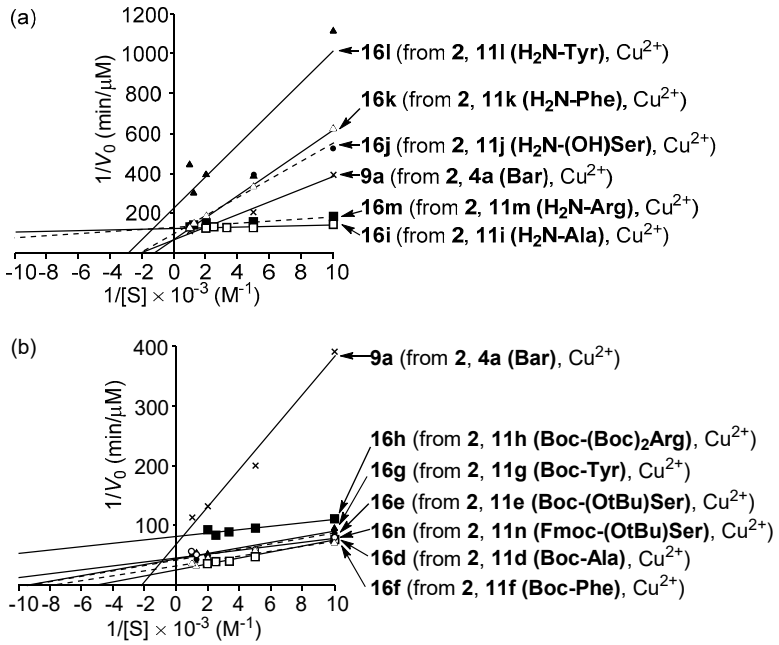

Figure 10. (**a**) Lineweaver–Burk plots for the hydrolysis of MNP catalyzed by **9a** (cross with plain line), **16i** (open squares with plain line), **16j** (closed circles with dashed line), **16k** (open triangles with plain line), **16l** (closed triangles with plain line), and **16m** (closed squares with dashed line). (**b**) Lineweaver–Burk plots for the hydrolysis of MNP by **9a** (crosses with plain line), **16d** (open squares with plain line), **16e** (closed circles with dashed line), **16f** (open triangles with dashed line), **16g** (closed triangles with plain line), **16h** (closed squares with plain line), and **16n** (open circles with plain line).

Table 2. Kinetics parameters for the hydrolysis of MNP by **8a** and AP in single-phase solvent system (10 mM HEPES buffer (pH 7.4) with I = 0.1 ($NaNO_3$)) at 37 °C, and **9a**, **10a**, **16b**, **16d**–**n**, **17d**, and **17f** in two-phase solvent system ($CHCl_3$/50 mM HEPES buffer (pH 7.4) with I = 0.1 ($NaNO_3$) (2/8)) at 37 °C.

Entry	Cat. [a]	V_{max} (μM min^{-1})	K_m (μM)	k (min^{-1}) [b]	K_i (μM)	K_m/K_i	CTN [c]
1	**8a** [d]	$(8.9 \pm 0.2) \times 10^{-2}$ [d]	$(4.1 \pm 0.3) \times 10^{2}$ [d]	$(2.2 \pm 0.2) \times 10^{-4}$ [d]	*ca.* 15 (mixed-type) [d]	*ca.* 27	0.4
2	**AP** [e]	1.3 ± 0.1 [e]	7 ± 4 [e]	$(2.9 \pm 1.8) \times 10^{-1}$ [e]	3 ± 1 (competitive) [e]	*ca.* 2.3	$>10^3$ [f]
3	**9a** [g]	$(1.4 \pm 0.4) \times 10^{-2}$ [g]	$(5.4 \pm 0.5) \times 10^{2}$ [g]	$(2.7 \pm 1.0) \times 10^{-5}$ [g]	*ca.* 15 (competitive) [g,h]	*ca.* 36	1.0
4	**10a** [h]	$(6.8 \pm 0.3) \times 10^{-2}$ [h]	$(3.8 \pm 0.2) \times 10^{2}$ [h]	$(1.8 \pm 0.2) \times 10^{-4}$ [h]	*ca.* 80 (mixed-type) [h]	*ca.* 4.8 [h]	~4
5	**16b** [i]	$(3.6 \pm 0.2) \times 10^{-2}$	$(2.5 \pm 0.3) \times 10^{2}$	$(1.4 \pm 0.3) \times 10^{-4}$	n.d. [j]	n.d. [j]	2.1
6	**16d** [i]	$(3.9 \pm 0.2) \times 10^{-2}$	$(1.9 \pm 0.1) \times 10^{2}$	$(2.1 \pm 0.2) \times 10^{-4}$	16 (competitive)	*ca.* 12	1.8
7	**16e** [i]	$(2.4 \pm 0.2) \times 10^{-2}$	$(1.1 \pm 0.1) \times 10^{2}$	$(2.2 \pm 0.4) \times 10^{-4}$	n.d. [j]	n.d. [j]	2.0
8	**16f** [i]	$(2.9 \pm 0.1) \times 10^{-2}$	$(1.2 \pm 0.1) \times 10^{2}$	$(2.4 \pm 0.3) \times 10^{-4}$	23 (competitive)	*ca.* 5.4	2.7
9	**16g** [i]	$(2.3 \pm 0.2) \times 10^{-2}$	$(1.0 \pm 0.1) \times 10^{2}$	$(2.4 \pm 0.4) \times 10^{-4}$	n.d. [j]	n.d. [j]	2.1
10	**16h** [i]	$(1.2 \pm 0.1) \times 10^{-2}$	33 ± 1	$(3.6 \pm 0.5) \times 10^{-4}$	n.d. [j]	n.d. [j]	1.1
11	**16i** [i]	$(8.1 \pm 0.2) \times 10^{-3}$	13 ± 1	$(6.0 \pm 0.4) \times 10^{-4}$	0.67 (competitive)	*ca.* 20	1.3
12	**16j** [i]	$(1.0 \pm 0.1) \times 10^{-2}$	$(4.7 \pm 0.2) \times 10^{2}$	$(2.2 \pm 0.2) \times 10^{-5}$	n.d. [j]	n.d. [j]	1.2
13	**16k** [i]	$(1.4 \pm 0.1) \times 10^{-2}$	$(7.6 \pm 0.2) \times 10^{2}$	$(1.9 \pm 0.2) \times 10^{-5}$	n.d. [j]	n.d. [j]	1.0
14	**16l** [i]	$(4.5 \pm 0.2) \times 10^{-3}$	$(3.5 \pm 0.1) \times 10^{2}$	$(1.3 \pm 0.1) \times 10^{-5}$	n.d. [j]	n.d. [j]	0.6
15	**16m** [i]	$(7.8 \pm 0.3) \times 10^{-3}$	40 ± 1	$(2.0 \pm 0.1) \times 10^{-4}$	n.d. [j]	n.d. [j]	1.2
16	**16n** [i]	$(2.2 \pm 0.2) \times 10^{-2}$	72 ± 2	$(3.0 \pm 0.3) \times 10^{-4}$	n.d. [j]	n.d. [j]	1.7
17	**17d** [i]	$(2.5 \pm 0.2) \times 10^{-2}$	$(1.2 \pm 0.1) \times 10^{2}$	$(2.2 \pm 0.4) \times 10^{-4}$	17 (mixed-type)	*ca.* 7.4	2.0
18	**17f** [i]	$(2.3 \pm 0.2) \times 10^{-2}$	47 ± 2	$(5.0 \pm 0.6) \times 10^{-4}$	5.7 (competitive)	*ca.* 8.3	2.3

[a] Cat = catalyst. [b] Calculated by eq. (1). [c] Catalytic turnover numbers determined at [MNP] = 1000 μM (see Figure 9). [d] From ref. 24 (in a single aqueous solution (10 mM HEPES buffer, pH 7.4 with I = 0.1 ($NaNO_3$)). [e] From ref. 19 (in a single aqueous solution (10 mM HEPES buffer, pH 7.4 with I = 0.1 ($NaNO_3$)). [f] Calculated from data in ref. 19. [g] From ref. 53. [h] From ref. 54. [i] Determined in $CHCl_3$/50 mM HEPES buffer (pH 7.4) with I = 0.1 ($NaNO_3$) (2/8). [j] Not determined.

The V_{max} and K_m values for **9a** were reported to be $(1.4 \pm 0.4) \times 10^{-2}$ μM min^{-1} and $(5.4 \pm 0.5) \times 10^2$ μM (entry 3 in Table 2), respectively, in a two-phase solvent system in our previous report [53]. Among **16b**, **16d–n**, **17d,** and **17f** tested in this work (entry 5–18 in Table 2), **16d** had the highest V_{max} (3.9×10^{-2} μM min^{-1}) (entry 6) and **16f** had the highest CTN (2.7) (entry 8).

The hydrolysis of MNP by **9a**, **16d**, **16f**, **16i**, **17d**, and **17f** in the presence of HPO_4^{2-}, a product and an inhibitor of MNP hydrolysis, was also carried out to determine the K_i values of HPO_4^{2-} as listed in Table 2. Interestingly, it was indicated that **9a**, **16d**, **16f**, and **16i** are inhibited by inorganic phosphate in a competitive manner and the K_i values for **16d** (16 μM) and **16f** (23 μM) (entries 6 and 8) was almost comparable to that for **9a** (*ca.* 15 μM) (entry 3). In contrast, the K_i value for **16i** is 0.67 μM (entry 11), which is much smaller than the others. We previously reported that smaller K_m/K_i values are good parameters for assessing the catalytic activity of the MNP catalysts [54]. For example, the K_m/K_i values for **10a** and **16f**, both of which function as catalysts are ca. 4.8 and 5.4 (entries 4 and 8), respectively, and these values are close to that for AP (*ca.* 2.3) (entry 2), and smaller than the corresponding values for **16d** (*ca.* 12) and **16i** (*ca.* 20) (entries 6 and 11), whose CTN values are 1.2–1.8.

Another important point is that **16d**, **16f**, **16i**, and **17f** are inhibited by HPO_4^{2-} in a competitive manner (entries 6, 8, 11, and 18), like that of AP. This type of inhibition is different from our previous supramolecular phosphatases such as **8a** (entry 1) that functions in a single-phase aqueous solution and **10a** that functions in a two-phase solvent system. Based on the above findings, we conclude that the quantitative distribution of **16d**, **16f**, **16i**, and **17f** in the organic phase (Table 1) adequately mimics the binding mode of AP with the substrate and inhibitors (MNP and HPO_4^{2-}, respectively, in this case).

The K_m values for **16d–h** (entries 6–10) (0.3–1.9×10^2 μM) are lower than that for **10a** (entry 4) (3.8×10^2 μM), although the K_i values for **16d**, **16f**, and **16i** (16, 23, and 0.67 μM, respectively) are also lower than that for **10a** (80 μM). The proposed structure of **16f** generated by BIOVIA Discovery Studio (Ver: 17.2.0) based on the crystal structure of **8a** (Figure 11a, in which Cu^{2+}-bound H_2O molecules are omitted for clarity) [24] suggests that the side chain of the **11f** unit in **16f** (yellow spheres) is located over the $Cu_2(\mu\text{-}OH)_2$ core, which results in the formation of a hydrophobic pocket similar to the active site of AP, as shown in Figure 11b,c. Therefore, we conclude that the hydrophobicity of supramolecular complexes is important in terms of improving the stabilization of the supermolecule–MNP complexes (i.e., the ES complexes) that have smaller K_m values and the effective extraction of MNP from the aqueous layer. Namely, the hydrophobic active site of the artificial supramolecular complexes is important for mimicking the hydrophobic active site of natural AP and hydrophobicity/hydrophilicity balance is important for catalytic activity.

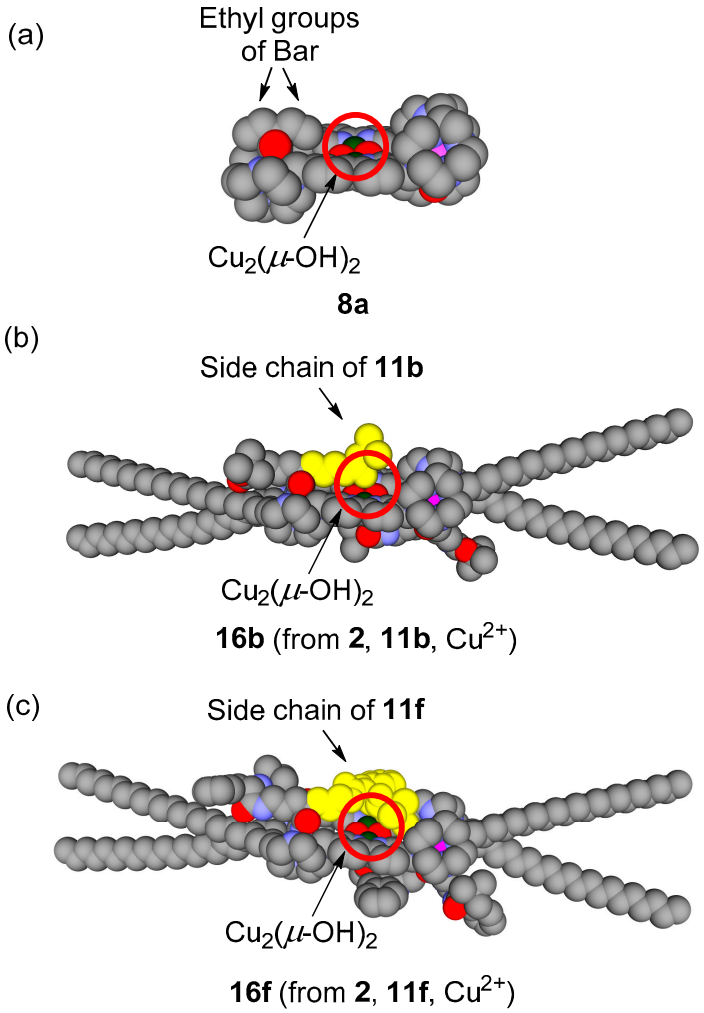

Figure 11. (**a**) X-ray crystal structure of **8a** and (**b** and **c**) proposed structures of **16b** and **16f** (yellow spheres indicate the side chains of the Bar units **11b** and **11f**).

4. Conclusions

In conclusion, we report on the design, and synthesis of Bar building units that are functionalized with amino acids and related units, with which many supramolecular complexes are formed by the 2:2:2 self-assembly of **2** (Zn_2L^2) and Cu^{2+} in a two-phase solvent system based on the structure of the active site of AP. The ease of functionalizing the barbital units allowed us to construct a series of various supramolecular complexes which were then used to assess their catalytic activity for the hydrolysis of MNP and related studies of the reaction mechanism. A comparison of the hydrolysis of MNP in a single-phase system and that in the two-phase system in the presence of **8**, **9**, **15**, or **16** strongly suggest that two-phase solvent system contributes to the improvement in the activity of MNP hydrolysis by reducing the product inhibition by HPO_4^{2-}. In addition, the hydrolysis of MNP by the hydrophobic supramolecular complexes follows Michaelis–Menten kinetics, and functionalization with Boc-protected phenylalanine (**16f**) results in a higher V_{max} and a lower K_m, and a greater k value than the corresponding values for **9a**. The K_m/K_i value for **16f** (*ca.* 5.4) is close to that for AP (*ca.* 2.3) and competitive inhibition by inorganic phosphate was observed, unlike for our previously reported complexes such as **10a**–**c**. We therefore conclude that the distribution of the $Cu_2(\mu\text{-}OH)_2$ active site of the supermolecules in both layers in the two-phase solvent system contributes to the improvement of catalytic turnover, and the formation of hydrophobic $Cu_2(\mu\text{-}OH)_2$ site mainly in organic layer appropriately mimics the binding mode of AP with the substrates (for the E–S complexation) and the

inhibitors (product inhibition). These findings should be highly useful for the design of more efficient catalysts in reference to biochemistry including enzymatic reactions.

Author Contributions: Y.M. carried out the synthesis of the barbital derivatives, UV/Vis titrations of supramolecular complexes, and hydrolysis of MNP by supramolecular complexes. A.B.R., H.I., and Y.H. carried out some of the measurements for the hydrolysis of MNP by the supramolecular complexes. Y.S. synthesized some of the barbital derivatives and carried out the hydrolysis of MNP by the supramolecular complexes. S.A. supervised all experiments and the preparation of the manuscript. All of the authors have read and approved the final version of the manuscript.

Funding: This research received no external funding.

Acknowledgments: This work was supported by grants-in-aid from the Ministry of Education, Culture, Sports, Science, and Technology (MEXT) of Japan (Nos. 24640156, 15K00408, 16K10396, and 17K08225 for S.A., and 17K08206 for Y.S.) and "Academic Frontiers" project for private universities: matching funds from MEXT, and the TUS (Tokyo University of Science) fund for strategic research areas. We wish to express our appreciation for the assistance of Fukiko Hasegawa (Faculty of Pharmaceutical Sciences, Tokyo University of Science) for obtaning the mass spectra, Noriko Sawabe for the NMR measurements, and Yuki Honda (Research institute for Science and Technology, Tokyo University of Science) for the elemental analyses.

Conflicts of Interest: The authors declare no conflict of interest.

References

1. Woodgett, J. *Protein Kinase Functions, Frontiers in Molecular Biology*; Oxford University Press: Oxford, UK, 2000.
2. Tibes, R.; Trent, J.; Kurzrock, R. Tyrosine kinase inhibitors and the dawn of molecular cancer therapeutics. *Annu. Rev. Pharmacol. Toxicol.* **2005**, *45*, 357–384. [CrossRef] [PubMed]
3. Jiao, Q.; Bi, L.; Ren, Y.; Song, S.; Wang, Q.; Wang, Y. Advances in studies of tyrosine kinase inhibitors and their acquired resistance. *Mol. Cancer* **2018**, *17*, 36. [CrossRef] [PubMed]
4. Coleman, J.E. Structure and mechanism of alkaline phosphatase. *Annu. Rev. Biophys. Biomol. Struct.* **1992**, *21*, 441–483. [CrossRef] [PubMed]
5. Millan, J.L. Alkaline phosphatases structure, substrate specificity and functional relatedness to other members of a large superfamily of enzymes. *Purinergic Signal.* **2006**, *2*, 335–341. [CrossRef] [PubMed]
6. O'Brien, P.J.; Herschlag, D. Functional interrelationships in the alkaline phosphatase superfamily: Phosphodiesterase activity of Escherichia coli alkaline phosphatase. *Biochemistry* **2001**, *40*, 5691–5699. [PubMed]
7. Denu, J.M.; Stuckey, J.A.; Saper, M.A.; Dixon, J.E. Form and function in protein dephosphorylation. *Cell* **1996**, *87*, 361–364. [CrossRef]
8. Kramer, R. Bioinorganic models for the catalytic cooperation of metal ions and functional groups in nuclease and peptidase enzymes. *Coord. Chem. Rev.* **1999**, *182*, 243–261. [CrossRef]
9. Cleland, W.W.; Hengge, A.C. Enzymatic mechanisms of phosphate and sulfate transfer. *Chem. Rev.* **2006**, *106*, 3252–3278. [CrossRef]
10. Kim, E.E.; Wyckoff, H.W. Reaction mechanism of alkaline phosphatase based on crystal structures. *J. Mol. Biol.* **1991**, *218*, 449–464. [CrossRef]
11. Kimura, E. Dimetallic hydrolases and their models. *Curr. Opin. Chem. Biol.* **2000**, *4*, 207–213. [CrossRef]
12. Aoki, S.; Kimura, E. *Bio-Coordination Chemistry in Comprehensive Coordination Chemistry II*; Que, L., Jr., Tolman, W.B., Eds.; Elsevier: Amsterdam, The Netherlands, 2003; Volume 8, pp. 601–640.
13. Seo, J.S.; Sung, N.-D.; Hynes, R.C.; Chin, J. Structure and reactivity of a dinuclear cobalt(III) complex with a bridging phosphate monoester. *Inorg. Chem.* **1996**, *35*, 7472–7473. [CrossRef]
14. Williams, N.H.; Lebuis, A.-M.; Chin, J. A structural and functional model of dinuclear metallophosphatases. *J. Am. Chem. Soc.* **1999**, *121*, 3341–3348. [CrossRef]
15. Williams, N.H.; Takasaki, B.; Wall, M.; Chin, J. Structure and nuclease activity of simple dinuclear metal complexes: Quantitative dissection of the role of metal ions. *Acc. Chem. Res.* **1999**, *32*, 485–493. [CrossRef]
16. Vance, D.H.; Czarnik, A.W. Functional group convergency in a binuclear dephosphorylation reagent. *J. Am. Chem. Soc.* **1993**, *115*, 12165–12166. [CrossRef]
17. Koike, T.; Inoue, M.; Kimura, E.; Shiro, M. Novel properties of cooperative dinuclear zinc(II) ions: The selective recognition of phosphomonoesters and their P−O ester bond cleavage by a new dinuclear zinc(II) cryptate. *J. Am. Chem. Soc.* **1996**, *118*, 3091–3099. [CrossRef]

18. Hettich, R.; Schneider, H.-J. Cobalt(III) polyamine complexes as catalysts for the hydrolysis of phosphate esters and of DNA. A measurable 10 million-fold rate increase. *J. Am. Chem. Soc.* **1997**, *119*, 5638–5647. [CrossRef]
19. Zulkefeli, M.; Suzuki, A.; Shiro, M.; Hisamatsu, Y.; Kimura, E.; Aoki, S. Selective hydrolysis of phosphate monoester by supramolecular phosphatase formed by the self-assembly of a Bis(Zn^{2+}-cyclen) complex, cyanuric acid, and copper in an aqueous solution (cyclen = 1, 4, 7, 10-Tetraazacyclododecane). *Inorg. Chem.* **2011**, *50*, 10113–10123. [CrossRef] [PubMed]
20. Der, B.S.; Edwards, D.R.; Kuhlman, B. Catalysis by a de novo zinc-mediated protein interface: Implications for natural enzyme evolution and rational enzyme engineering. *Biochemistry* **2012**, *51*, 3933–3940. [CrossRef]
21. Zhang, X.; Zhu, Y.; Zheng, X.; Phillips, D.L.; Zhao, C. Mechanistic investigation on the cleavage of phosphate monoester catalyzed by unsymmetrical macrocyclic dinuclear complexes: The selection of metal centers and intrinsic flexibility of the ligand. *Inorg. Chem.* **2014**, *53*, 3354–3361. [CrossRef]
22. Xue, S.-S.; Zhao, M.; Ke, Z.-F.; Cheng, B.-C.; Su, H.; Cao, H.; Cao, K.C.; Wang, J.; Ji, L.-N.; Mao, Z.-W. Enantioselective hydrolysis of amino acid esters promoted by Bis(ß-cyclodextrin) copper complexes. *Sci. Rep.* **2016**, *6*, 22080. [CrossRef]
23. Lin, Y.-W. Rational design of metalloenzymes: From single to multiple active sites. *Coord. Chem. Rev.* **2017**, *336*, 1–27. [CrossRef]
24. Zulkefeli, M.; Hisamatsu, Y.; Suzuki, A.; Miyazawa, Y.; Shiro, M.; Aoki, S. Supramolecular phosphatases formed by the self-assembly of the Bis(Zn^{2+}-cyclen) complex, copper(II), and barbital derivatives in water. *Chem. Asian J.* **2014**, *9*, 2831–2841. [CrossRef] [PubMed]
25. Coon, M.M.; Rebek, J., Jr. Self-assembling capsules. *Chem. Rev.* **1997**, *97*, 1647–1668. [CrossRef]
26. Fujita, M. *Molecular Self-Assembly Organic Versus Inorganic Approaches*; Springer: Berlin, Germany, 2000; Volume 96.
27. Breit, B. Supramolecular approaches to generate libraries of chelating bidentate ligands for homogeneous catalysis. *Angewandte Chem. Int. Ed.* **2005**, *44*, 6816–6825. [CrossRef]
28. Kleij, A.W.; Reek, J.N.H. Ligand-template directed assembly: An efficient approach for the supramolecular encapsulation of transition-metal catalysts. *Chem. Eur. J.* **2006**, *12*, 4218–4227. [CrossRef] [PubMed]
29. Oshovsky, G.V.; Reinhoudt, D.N.; Verboom, W. Supramolecular chemistry in water. *Angewandte Chem. Int. Ed.* **2007**, *46*, 2366–2393. [CrossRef] [PubMed]
30. Hannon, M.J. Supramolecular DNA recognition. *Chem. Soc. Rev.* **2007**, *36*, 280–295. [CrossRef]
31. Van Leeuwen, P.W.N.M. *Supramolecular Catalysis*; Wiley-VCH: New York, NY, USA, 2008.
32. Koblenz, T.S.; Wassenaar, J.; Reek, J.N.H. Reactivity within a confined self-assembled nanospace. *Chem. Soc. Rev.* **2008**, *37*, 247–262. [CrossRef]
33. Suzuki, K.; Tominaga, M.; Kawano, M.; Fujita, M. Self-assembly of an M_6L_{12} coordination cube. *Chem. Commun.* **2009**, 1638–1640. [CrossRef]
34. Northrop, B.H.; Zheng, Y.-R.; Chi, K.-W.; Stang, P.J. Self-organization in coordination-driven self-assembly. *Acc. Chem. Res.* **2009**, *42*, 1554–1563. [CrossRef]
35. Leung, K.C.-F.; Chak, C.-P.; Lo, C.-M.; Wong, W.-Y.; Xuan, S.; Cheng, C.H.K. pH-Controllable supramolecular systems. *Chem. Asian J.* **2009**, *4*, 364–381. [CrossRef] [PubMed]
36. Yoshizawa, M.; Klosterman, J.K.; Fujita, M. Functional molecular flasks: New properties and reactions within discrete, self-assembled hosts. *Angewandte Chem. Int. Ed.* **2009**, *48*, 3418–3438. [CrossRef] [PubMed]
37. Yoshizawa, M.; Fujita, M. Development of unique chemical phenomena within nanometer-sized, self-assembled coordination hosts. *Bull. Chem. Soc. Jpn.* **2010**, *83*, 609–618. [CrossRef]
38. Trabolsi, A.; Khashab, N.; Fahrenbach, A.C.; Friedman, D.C.; Colvin, M.T.; Coti, K.K.; Benitez, D.; Tkatchouk, E.; Olsen, J.-C.; Belowich, M.E.; et al. Radically enhanced molecular recognition. *Nat. Chem.* **2010**, *2*, 42–49. [CrossRef]
39. Meeuwissen, J.; Reek, J.N.H. Supramolecular catalysis beyond enzyme mimics. *Nat. Chem.* **2010**, *2*, 615–621. [CrossRef]
40. Ma, Z.; Moulton, B. Recent advances of discrete coordination complexes and coordination polymers in drug delivery. *Coord. Chem. Rev.* **2011**, *255*, 1623–1641. [CrossRef]
41. Aoki, S.; Zulkefeli, M.; Hisamatsu, Y.; Kitamura, M. Supramolecular host and catalysts formed by the synergistic molecular assembly of multinuclear zinc(II) complexes in aqueous solution. In *Synergy in Supramolecular Chemistry*; Nabeshima, T., Ed.; CRC: Boca Raton, FL, USA, 2015; pp. 33–56.

42. Kimura, E.; Koike, T.; Aoki, S. Evolution of ZnII-macrocyclic polyamines to biological probes and supramolecular assembly elements. In *Macrocyclic and Supramolecular Chemistry: How Izatt-Christensen Award Winners Shaped the Field*; Izatt, R.M., Ed.; John Wiley & Sons: Hoboken, NJ, USA, 2016; pp. 417–445.
43. Gibb, C.L.D.; Gibb, B.C. Well-defined, organic nanoenvironments in water: The hydrophobic effect drives a capsular assembly. *J. Am. Chem. Soc.* **2004**, *126*, 11408–11409. [CrossRef] [PubMed]
44. Slagt, V.F.; Kamer, P.C.J.; Van Leeuwen, P.W.N.M.; Reek, J.N.H. Encapsulation of transition metal catalysts by ligand-template directed assembly. *J. Am. Chem. Soc.* **2004**, *126*, 1526–1536. [CrossRef] [PubMed]
45. Kuil, M.; Soltner, T.; Van Leeuwen, P.W.N.M.; Reek, J.N.H. High-precision catalysts: Regioselective hydroformylation of internal alkenes by encapsulated rhodium complexes. *J. Am. Chem. Soc.* **2006**, *128*, 11344–11345. [CrossRef] [PubMed]
46. Neelakandan, P.P.; Hariharan, M.; Ramaiah, D. A supramolecular ON−OFF−ON fluorescence assay for selective recognition of GTP. *J. Am. Chem. Soc.* **2006**, *128*, 11334–11335. [CrossRef] [PubMed]
47. Nishioka, Y.; Yamaguchi, T.; Yoshizawa, M.; Fujita, M. Unusual [2+4] and [2+2] cycloadditions of arenes in the confined cavity of self-assembled cages. *J. Am. Chem. Soc.* **2007**, *129*, 7000–7001. [CrossRef] [PubMed]
48. Natarajan, A.; Kaanumalle, L.S.; Jockusch, S.; Gibb, C.L.D.; Gibb, B.C.; Turro, N.J.; Ramamurthy, V. Controlling photoreactions with restricted spaces and weak intermolecular forces: Exquisite selectivity during oxidation of olefins by singlet oxygen. *J. Am. Chem. Soc.* **2007**, *129*, 4132–4133. [CrossRef] [PubMed]
49. Sawada, T.; Yoshizawa, M.; Sato, S.; Fujita, M. Minimal nucleotide duplex formation in water through enclathration in self-assembled hosts. *Nat. Chem.* **2009**, *1*, 53–56. [CrossRef] [PubMed]
50. Gianneschi, N.C.; Nguyen, S.T.; Mirkin, C.A. Signal amplification and detection via a supramolecular allosteric catalyst. *J. Am. Chem. Soc.* **2005**, *127*, 1644–1645. [CrossRef] [PubMed]
51. Lee, S.J.; Cho, S.H.; Mulfort, K.L.; Tiede, D.M.; Hupp, J.T.; Nguyen, S.T. Cavity-tailored, self-sorting supramolecular catalytic boxes for selective oxidation. *J. Am. Chem. Soc.* **2008**, *130*, 16828–16829. [CrossRef]
52. Murase, T.; Horiuchi, S.; Fujita, M. Naphthalene Diels−Alder in a self-assembled molecular flask. *J. Am. Chem. Soc.* **2010**, *132*, 2866–2867. [CrossRef]
53. Hisamatsu, Y.; Miyazawa, Y.; Yoneda, K.; Miyauchi, M.; Zulkefeli, M.; Aoki, S. Supramolecular complexes formed by the self-assembly of hydrophobic Bis(Zn^{2+}-cyclen) complexes, copper, and Di- or Triimide units for the hydrolysis of phosphate Mono- and diesters in two-phase solvent systems (Cyclen = 1, 4, 7, 10-Tetraazacyclododecane). *Chem. Pharm. Bull.* **2016**, *64*, 451–464. [CrossRef]
54. Rahman, A.B.; Imafuku, Y.; Miyazawa, Y.; Kalfe, A.; Sakai, H.; Saga, Y.; Aoki, S. Catalytic hydrolysis of phosphate monoester by supramolecular phosphatases formed from a monoalkylated dizinc(II) complex, cyclic diimide units, and copper(II) in two-phase solvent system. *Inorg. Chem.* **2019**, *58*, 5603–5616. [CrossRef]
55. Nilsson, B.L.; Soellner, M.B.; Raines, R.T. Chemical synthesis of proteins. *Annu. Rev. Biophys. Biomol. Struct.* **2005**, *34*, 91–118. [CrossRef]
56. Van Berkel, S.S.; Van Eldijk, M.B.; Van Hest, J.C.M. Staudinger ligation as a method for bioconjugation. *Angewandte Chem. Int. Ed.* **2011**, *50*, 8806–8827. [CrossRef]
57. Sagel, I.H. *Biochemical Calculations*, 2nd ed.; John Wiley & Sons: New York, NY, USA, 1976.